

UNCLASSIFIED

AD NUMBER
AD872980
NEW LIMITATION CHANGE
TO Approved for public release, distribution unlimited
FROM Distribution authorized to U.S. Gov't. agencies and their contractors; Administrative/Operational use; Aug 1970. Other requests shall be referred to Air Force Aero Propulsion Laboratory, [APFL], Wright-Patterson Air Force Base, Ohio 45433.
AUTHORITY
AFAPL, ltr, 2 Sept 1971

THIS PAGE IS UNCLASSIFIED

AD No. — AD872980

AFAPL-TR-65-45
Part IX

30

ROTOR-BEARING DYNAMICS DESIGN TECHNOLOGY

Part IX: Thrust Bearing Effects on Rotor Stability

DDS FILE COPY

R. Gundiff
J. Vohr

AUG 14 1970

[Handwritten signature]

Mechanical Technology Incorporated

TECHNICAL REPORT AFAPL-TR-65-45, PART IX

August 1970

This document is subject to special export controls and each transmittal to foreign governments or foreign national may be made only with prior approval of the Air Force Aero Propulsion Laboratory (APFL), Wright-Patterson Air Force Base, Ohio 45433.

Air Force Aero Propulsion Laboratory
Air Force Systems Command
Wright-Patterson Air Force Base, Ohio

Best Available Copy

NOTICE

When Government drawings, specifications, or other data are used for any purpose other than in connection with a definitely related Government procurement operation, the United States Government thereby incurs no responsibility nor any obligation whatsoever; and the fact that the government may have formulated, furnished, or in any way supplied the said drawings, specifications, or other data, is not to be regarded by implication or otherwise as in any manner licensing the holder or any other person or corporation, or conveying any rights or permission to manufacture, use, or sell any patented invention that may in any way be related thereto.

This document is subject to special export controls and each transmittal to foreign governments of foreign nationals may be made only with prior approval of the Air Force Aero Propulsion Laboratory (APFL), Wright-Patterson Air Force Base, Ohio 45433.

DATE RECEIVED	
APPROVED FOR EXPORT	
CLASSIFICATION	
DATE	
2	

Copies of this report should not be returned unless return is required by security considerations, contractual obligations, or notice on a specific document.

0 cldslawA for 7

AFAPL-TR-65-45

Part IX

ROTOR-BEARING DYNAMICS DESIGN TECHNOLOGY

**Part IX: Thrust Bearing Effects
on Rotor Stability**

R. Cundiff

J. Vohr

Mechanical Technology Incorporated

TECHNICAL REPORT AFAPL-TR-65-45, PART IX

August 1970

This document is subject to special export controls and each transmittal to foreign governments or foreign national may be made only with prior approval of the Air Force Aero Propulsion Laboratory (APFL), Wright-Patterson Air Force Base, Ohio 45433.

**Air Force Aero Propulsion Laboratory
Air Force Systems Command
Wright-Patterson Air Force Base, Ohio**

Best Available Copy

FOREWORD

This report was prepared by Mechanical Technology Incorporated, 968 Albany-Shaker Road, Latham, New York 12110 under USAF Contract No. AF33(615)-3238. The contract was initiated under Project No. 3048, Task No. 304806. The work was administered under the direction of the Air Force Aero Propulsion Laboratory, with Mr. M. Robin Chasman and Mr. Everett A. Lake (APFL) acting as project engineer.

This report covers work conducted from 1 October 1968 to 1 January 1970.

This report was submitted by the authors on June 5, 1970.

This report is Part IX of final documentation issued in multiple parts.

Publication of this report does not constitute Air Force approval of the report's findings or conclusions. It is published only for the exchange and stimulation of ideas.



HOWARD F. JONES, Chief
Lubrication Branch
Fuel, Lubrication & Hazards Division
Air Force Aero Propulsion Laboratory

ABSTRACT

This volume presents a study conducted to determine the effects thrust bearings have on rotor-bearing stability. A computer program was written in order to study these effects and permits the inclusion of the thrust bearing characteristics into the rotor system. A manual is provided for the program, containing a listing of the program and detailed instructions for preparation of input data. A technique is also presented which permits the user a convenient method of evaluating the stability of a rotor system with and without the thrust bearing data. Extensive design data are presented for gas-lubricated, externally pressurized thrust bearings.

This abstract is subject to special export controls and each transmittal to foreign governments or foreign nationals may be made only with prior approval of the Air Force Aero Propulsion Laboratory (APFL), Wright-Patterson Air Force Base, Ohio 45433.

TABLE OF CONTENTS

	<u>Page</u>
I. INTRODUCTION	1
II. THE DETERMINATION OF THRESHOLD SPEED FOR WHIRL INSTABILITY OF A ROTOR	2
1. General Discussion	2
2. Analysis of Stability of Arbitrary, Non-Symmetrical Rotor....	10
3. Determination of Rotor-Bearing Stability by Means of Critical Speed Maps.....	13
III. EFFECT OF THRUST BEARING STIFFNESS AND DAMPING ON ROTOR-BEARING STABILITY	18
1. Discussion.....	18
2. Sample Calculations.....	22
IV. ANGULAR STIFFNESS COEFFICIENTS FOR HYDROSTATIC THRUST BEARINGS ...	50
APPENDIX I: Computer Program - PN400 - The Threshold of Instability of a Flexible Rotor in Fluid Film Bearings..	61
REFERENCES	86

ILLUSTRATIONS

<u>Figure</u>	<u>Page</u>
1. Coordinate System for Forces and Displacement.....	4
2. Loci of Roots for Real and Imaginary Parts of Equation (10).....	9
3. Sign Convention for Amplitude, Slope, Bending Moment and Shear Force Illustrated in x-z Plane.....	11
4. Coordinate Axis System.....	19
5. Conical Instability Rotor Model 1.....	23
6. Conical Instability Rotor Model 2.....	24
7. Critical Speed Map of Rotor 1.....	33
8. Loci for Roots of Real and Imaginary Parts of Stability Determinant.....	35
9. Loci for Roots of Real and Imaginary Parts of Stability Determinant.....	40
10. Critical Speed Map of Rotor 2.....	44
11. Loci of Roots for Real and Imaginary Parts of Stability Determinant.....	46
12. Sketch of Hydrostatic Thrust Bearing.....	51
13. Hydrostatic Thrust Bearing, $R_o/R_i = 1.25$. Dimensionless Angular Stiffness vs. Restrictor ¹ Coefficient.....	54
14. Hydrostatic Thrust Bearing, $R_o/R_i = 1.5$. Dimensionless Angular Stiffness vs. Restrictor ¹ Coefficient.....	55
15. Hydrostatic Thrust Bearing, $R_o/R_i = 2$. Dimensionless Angular Stiffness vs. Restrictor ¹ Coefficient.....	56
16. Hydrostatic Thrust Bearing, $R_o/R_i = 3$. Dimensionless Angular Stiffness vs. Restrictor ¹ Coefficient.....	57
17. Dynamic Angular Stiffness for the Hydrostatic Thrust Bearing $R_o/R_i = 1.5$. Inherent Compensation.....	58
18. Dynamic Angular Stiffness for the Hydrostatic Thrust Bearing $R_o/R_i = 3$. Inherent Compensation.....	59
19. Minimum Number of Feeder Holes.....	60

SYMBOLS

a	Orifice radius, inch
a_{mn}	Dynamic influence coefficients
A	Defined by Eq. (20)
B	Single effective bearing damping, defined by Eq. (19), lbs·sec/in
B_{major}	Maximum value of B , lbs·sec/in
B_{minor}	Minimum value of B , lbs·sec/in
$B_{xx}, B_{xy}, B_{yx}, B_{yy}$	Dynamic bearing damping coefficients, lbs·sec/inch
\bar{B}	Dimensionalized bearing damping coefficient = $G\omega B/P_a LD$
C	Radial clearance, inch
D	Bearing diameter, inch
$D_{xx}, D_{xy}, D_{yx}, D_{yy}$	Dynamic angular bearing damping coefficients, lbs·sec·inch./radians
e	Steady-state bearing eccentricity, inch
F_x, F_y	Bearing fluid film forces, lbs.
$G_{xx}, G_{xy}, G_{yx}, G_{yy}$	Dynamic angular bearing stiffness coefficients, lbs·inch./radian
i	= $\sqrt{-1}$
$Im\{\}$	Imaginary part of complex expression
K	Single effective spring stiffness, defined by Eq. (18), lb/in.
K_{major}	Maximum value of K , lb/in.
K_{minor}	Minimum value of K , lb/in.
$K_{xx}, K_{xy}, K_{yx}, K_{yy}$	Dynamic bearing stiffness coefficients, lbs/inch
\bar{K}	Dimensionalized stiffness coefficient = $CK/P_a LD$

L	Bearing length, inch
L	Half bearing span length, inch = $L_1 + L_2$
L_1	Distance from rotor C.G. to centerline of bearing number 1
L_2	Distance from rotor C.G. to centerline of bearing number 2
M	Journal bearing mass (half rotor mass for rigid rotor), lbs·sec ² /inch
M_c	Critical mass per bearing, lbs·sec ² /inch
M_x, M_y	x and y-component of rotor bending moment to the left of a rotor mass station, lbs·inch
M'_x, M'_y	x and y-component of rotor bending moment to the right of the rotor mass station, lbs·inch
n	Number of feeder holes
P_a	Ambient pressure, psia
P_s	Supply pressure, psia
R	Bearing radius, inch
Re()	Real part of complex expression
R_o	Outer radius of thrust bearing, inch
R_i	Inner radius of thrust bearing, inch
R	Gas constant, inch ² /sec ² °R
T	Temperature of gas lubricant, °R
t	Time, seconds
V_x, V_m	x and y-component of rotor shear force to the left of a rotor mass station, lbs.
V'_x, V'_y	x and y-component of rotor shear force to the right of a rotor mass station, lbs.
W	Static load on bearing, lbs.

W_x, W_y	External forces on rotor in x and y direction, lbs.
$Z_{xx}, Z_{xy}, Z_{yx}, Z_{yy}$	Complex notation of stiffness and damping axial coordinate, inch
x, y	Rotor amplitudes, inch
x_c, x_s	Cosine and sine component of rotor x-amplitude, inch
y_c, y_s	Cosine and sine component of rotor y-amplitude, inch
z	Axial coordinate, inch
γ	= v/ω , whirl frequency ratio
Δ	Complex deterministic equation
Δ_c	= $\text{Re}(\Delta)$, real part of complex equation
Δ_s	= $\text{Im}(\Delta)$, imaginary part of complex equation
δ	= a^2/dC , inherent compensation factor
ϵ_B	= e/C , eccentricity ratio for bearing
θ	Angular displacement of thrust bearing in x-z plane, radian
Λ	= $\frac{12\mu\omega N}{P_a} \left(\frac{R_o}{C} \right)^2$, Compressibility number
Λ_s	= $\frac{6\mu\omega a^2 \sqrt{RT}}{P_s C^3 \sqrt{1 + \delta^2}}$, restrictor coefficient
μ	Lubricant viscosity, lbs·sec/in ²
v	Whirl frequency, rad/sec
v_c	Critical whirl frequency at threshold of instability, rad/sec
σ	= $\frac{12\mu v}{P_a} \left(\frac{R_1 R_o}{C^2} \right)$, Squeeze number

ψ	Angular displacement of thrust bearing in y-z plane, radi
ϕ	Bearing attitude angle, deg.
ψ	Angular displacement of thrust bearing in y-z plane, rad.
ω	Journal angular velocity, rad/sec
ω_T	Journal angular velocity at threshold, rad/sec

Subscripts

B	Bearing
C,S	Cosine and sine component (real and imaginary part)
C	Critical value
e	Effective
j	Journal bearing
m	Number of total rotor stations
n	Rotor station number
T	Thrust bearing
x,y	x and y-direction

Superscripts

dot	Time derivative
bar	Dimensionless quantity

SECTION I
INTRODUCTION

For rotors possessing a high degree of dissymmetry or for rather short rotors the instability whirl motion will have a substantial conical whirl component. Under such conditions the dynamic forces imposed on the rotor by the thrust bearing will have an important effect on the dynamical characteristics and the stability of the rotor-bearing system.

The purpose of the study described in this report was to develop the technology for determining effects of thrust bearing forces on the stability of rotors supported in fluid film bearings and to assess the significance of this effect on rotors of practical design. To this end, a computer program was developed to perform many of the complex calculations necessary for determination of the stability limits of complicated rotor-bearing systems which takes account of effects of thrust bearing stiffness and damping. This computer program is an extension and modification of a similar program developed in an earlier task performed under contract AF33(615) 3238 (Ref. 1). A complete description of the program including a computer listing is provided in the present report.

The present report provides angular stiffness data for hydrostatic thrust bearing geometries for use in the determination of rotor stability. Also a useful, simplified method for determining stability of rotors supported on bearings all of which are the same is described. Finally, several numerical examples of the calculation of thrust bearing effects on rotor stability are presented and the significance of these effects is discussed.

SECTION II

THE DETERMINATION OF THRESHOLD SPEED FOR WHIRL INSTABILITY OF A ROTOR

1. General Discussion

As is well established, a fluid film bearing supporting a rotor may be likened to a spring-dashpot system in that the bearing reaction to small displacements may be expressed in terms of stiffness and damping coefficients. A mass supported by springs has a number of natural spring-mass frequencies depending on the complexity of the spring system and the possible modes of motion of the mass. If any mode of motion is excited at the natural frequency by an external harmonic force, then the response of the system will be at a maximum but, if the system possesses effective damping for this mode of excitation, then the response will be bounded and the system will not be unstable. If, on the other hand, the natural frequency of a mode of motion corresponds to a condition where the effective damping of the system is negative, then the motion of the system at that frequency will increase without bound without any external excitation, and the system is considered as being unstable, i.e. subject to self-excited vibration. If a natural frequency occurs at a condition of zero damping, then the system can be said to be at the threshold of instability, where infinitesimally small exciting forces applied over a period of time will result in ever increasing amplitudes of response.

The so-called critical speeds of a rotor-bearing system refer to resonant responses of the system to unbalance forces of the system which, by their nature, are applied at a frequency synchronous with the rotational speed of the shaft. Since fluid film bearings in general have positive damping to synchronous speed oscillations, critical speeds are not instabilities but simply represent a condition of large resonant response to inherent unbalance forces. Fluid film bearings, however, do have an effective damping to various modes of motion which does tend toward zero when the motion occurs at some fraction of the running speed, usually at half the running speed. Thus, as the running speed of a rotor increases beyond the first critical speed or natural frequency speed, the rotor will begin to approach the condition where the first resonant or natural frequency of the system will coincide with the fractional frequency at which effective damping goes to zero. When this coincidence occurs, the rotor is said to have reached the whirl threshold speed. A

further increase in rotor speed usually results in a very rapid growth of whirl amplitude and, in almost all cases, the whirl threshold speed represents the upper limit for safe operation of the rotor.

We might note at this time that because effective damping of fluid film bearings tends toward zero for half-frequency oscillations, the rule of thumb has arisen that the threshold of instability is reached at about twice the first critical speed of the rotor. The basis for this rule of thumb will be examined in more detail in subsection 3 where there is discussed a procedure for using critical speed maps for predicting threshold of whirl instability.

Having briefly discussed the qualitative nature of whirl instability and its distinction from critical speeds, we will now proceed to show the nature of the linearized analysis required to determine the whirl threshold speed. In the illustrative treatment below, we shall consider only the translatory mode of a symmetric rotor supported on two identical bearings. The more general case of the translatory, conical and bending modes of a non-symmetric rotor will be considered in subsection 2. For this general case, determination of whirl threshold speed requires use of the computer program developed in this study. For the simpler case presented below, whirl threshold speed can be determined analytically.

For the translatory mode of a rigid symmetric rotor the gravity and inertia (D'Alembert) forces are equally borne by the two bearings. The kinematic relationships between the rotor and stator bearing surfaces at one bearing are at every instant identical as those of the other. It is therefore only necessary to consider the motion of one journal which has a mass equal to one-half the rotor mass. Let the rotor mass be $2M$ and the journal center amplitudes be x and y .

At any given rotor speed and with a known static load on the bearing, the journal center occupies a certain unique equilibrium position relative to the bearing center. When the journal whirls around its equilibrium position in a small orbit, hydrodynamic bearing forces are generated in the bearing fluid film. These dynamic forces can be expressed in a linearized form by expanding the film forces into a first order Taylor series. With the bearing fluid film dynamic forces represented by F_x and F_y and with the dynamic external forces on the rotor represented by W_x and W_y as shown in Fig. 1, the linearized equation of motion become:

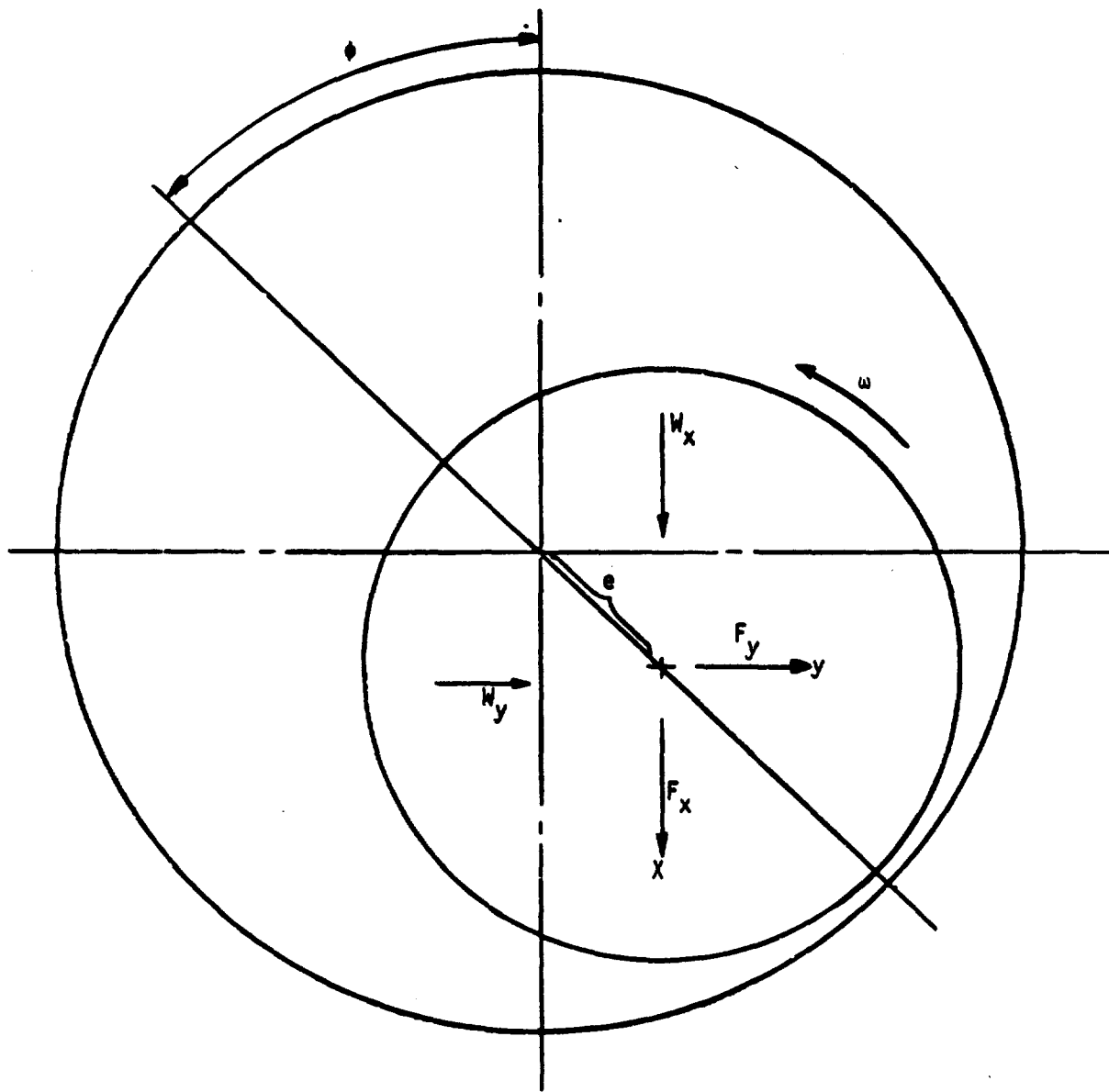


Fig. 1 Coordinate System for Forces and Displacements

$$M \frac{d^2 x}{dt^2} = F_x + W_x = -K_{xx} x - B_{xx} \dot{x} - K_{xy} y - B_{xy} \dot{y} + W_x \quad (1)$$

$$M \frac{d^2 y}{dt^2} = F_y + W_y = -K_{yy} y - B_{yy} \dot{y} - K_{yx} x - B_{yx} \dot{x} + W_y$$

where x and y are the whirl amplitudes measured from the static equilibrium position, t is time, and the four radial stiffness coefficients and the four radial damping coefficients are computed from the lubrication equation (Reynolds equation) as described in Ref. 2. For a given bearing geometry and known lubricant properties, the eight coefficients are functions of the bearing load and the rotor speed and, if the lubricant is compressible like a gas, they are also functions of the whirl frequency. At the threshold of instability, x and y are pure harmonic motions and can be conveniently expressed in terms of the whirl frequency ν :

$$x = x_c \cos(\nu t) - x_s \sin(\nu t) \quad (2)$$

$$y = y_c \cos(\nu t) - y_s \sin(\nu t)$$

These equations can also be expressed in complex form:

$$x = \text{Re} \left\{ (x_c + ix_s) e^{i\nu t} \right\} = x_c \cos(\nu t) - x_s \sin(\nu t) \quad (3)$$

$$y = \text{Re} \left\{ (y_c + iy_s) e^{i\nu t} \right\} = y_c \cos(\nu t) - y_s \sin(\nu t)$$

where $\text{Re} \{ \}$ indicates that only the real part of the complex equation is applicable. For convenience the $\text{Re} \{ \}$ notation is dropped and Eq. (3) is expressed:

$$x = (x_c + ix_s) e^{i\nu t} \quad (4)$$

$$y = (y_c + iy_s) e^{i\nu t}$$

When these equations are used in the analysis their complete meaning is defined by Eq. (3). Time derivatives can also be carried out in the complex notation,

bearing in mind that only the real part is of significance; e.g.

$$\begin{aligned} \dot{x} &= \frac{\partial}{\partial t} \operatorname{Re} \left\{ (x_c + ix_s) e^{i\omega t} \right\} \\ &= \operatorname{Re} \left\{ (x_c + ix_s) \frac{\partial}{\partial t} (e^{i\omega t}) \right\} \\ &= \operatorname{Re} \left\{ i\omega (x_c + ix_s) e^{i\omega t} \right\} \\ &= -\omega x_c \sin \omega t - \omega x_s \cos \omega t \end{aligned}$$

By differentiating Eqs. (4) and substituting into Eqs. (1) the equations of motion can be written:

$$M \ddot{x} = -Z_{xx} x - Z_{xy} y + W_x \quad (5)$$

$$M \ddot{y} = -Z_{yx} x - Z_{yy} y + W_y$$

where:

$$Z_{xx} = K_{xx} + i\gamma \omega B_{xx} \quad (\text{Similarly for } Z_{xy}, Z_{yx}, Z_{yy}) \quad (6)$$

$$= K_{xx} + i\gamma \omega B_{xx}$$

$$\gamma = \nu/\omega \quad (7)$$

Here, ω is the angular speed of rotation and γ is the ratio of the whirl frequency to the rotational frequency. In this form, the equations are equally valid for an incompressible and a compressible lubricant. In matrix form Eqs. (5) can be expressed:

$$\begin{Bmatrix} (Z_{xx} - Mv^2) & Z_{xy} \\ Z_{yx} & (Z_{yy} - Mv^2) \end{Bmatrix} \begin{Bmatrix} x \\ y \end{Bmatrix} = \begin{Bmatrix} W_x \\ W_y \end{Bmatrix} \quad (8)$$

For the rotor-bearing represented by Eq. (8) to be unstable, it is necessary and sufficient that Eq. (8) yield a non-zero solution for the amplitudes x and y when the external forces W_x and W_y are zero, i.e. for the system to be unstable a non-trivial solution to Eq. (9) below must be found.

$$\begin{Bmatrix} (Z_{xx} - Mv^2) & Z_{xy} \\ Z_{yx} & (Z_{yy} - Mv^2) \end{Bmatrix} \begin{Bmatrix} x \\ y \end{Bmatrix} = 0 \quad (9)$$

For a non-trivial solution to exist, the determinant of the matrix must vanish. Setting both the real and imaginary parts of the determinant to zero gives;

$$\Delta = \Delta_c + i\Delta_s = (Z_{xx} - Mv^2)(Z_{yy} - Mv^2) - Z_{xy} Z_{yx} = 0 \quad (10)$$

$$\begin{aligned} \Delta_c &= \text{Re} \{ \Delta \} = (K_{xx} - Mv^2)(K_{yy} - Mv^2) - K_{xy} K_{yx} \\ &- \gamma^2 (\omega B_{xx} \omega B_{yy} - \omega B_{xy} \omega B_{yx}) = 0 \end{aligned} \quad (11)$$

$$\begin{aligned} \Delta_s &= \text{Im} \{ \Delta \} = \gamma \left[(K_{xx} - Mv^2) \omega B_{yy} + (K_{yy} - Mv^2) \omega B_{xx} \right. \\ &\left. - K_{xy} \omega B_{yx} - K_{yx} \omega B_{xy} \right] = 0 \end{aligned} \quad (12)$$

Thus, when both the real and imaginary parts of the determinant vanish simultaneously harmonic motion or whirl is present and this whirl is referred to as rotor instability. Every combination of γ and ω satisfying either Eq. (11) or Eq. (12) can be represented by a point in a γ - ω plot. Typically the loci of these points appear as shown in Fig. 2.

Eqs. (11) and (12) contain two unknowns, the whirl frequency ratio, γ , and the angular speed of rotation, ω . For incompressible fluids, the eight dynamic film coefficients are independent of γ , thus Eqs. (11) and (12) may be solved yielding two expressions for Mv^2 and γ^2 .

$$Mv^2 = \frac{K_{xx} \omega_B_{yy} + K_{yy} \omega_B_{xx} - K_{xy} \omega_B_{yx} - K_{yx} \omega_B_{xy}}{\omega_B_{xx} + \omega_B_{yy}} \quad (13)$$

$$\gamma^2 = \frac{(K_{xx} - Mv^2)(K_{yy} - Mv^2) - K_{xy} K_{yx}}{\omega_B_{xx} \omega_B_{yy} - \omega_B_{xy} \omega_B_{yx}} \quad (14)$$

At a given rotational speed and load and with the eight coefficients known, Mv^2 may be calculated from Eq. (13) and when substituted into Eq. (14) gives the whirl frequency ratio squared value γ^2 . Two methods of establishing an instability criteria may be obtained from these two values. First, the actual mass at the journal bearing may be substituted into the Mv^2 term to solve for the v^2 value which when substituted into the γ^2 value yields the apparent threshold frequency. If this threshold frequency is identical to the rotor speed at which the coefficients were based then the threshold speed has been obtained. The second method substitutes the rotor speed, ω , in the γ^2 term to find the whirl frequency v which, when substituted into the Mv^2 term, yields a critical mass M_c for onset of instability. If the actual journal bearing mass M is less than M_c , then the system is stable; if M is greater than M_c , the system is

unstable. The mathematical derivation of this stability criterion is given in Ref. 4.

From compressible fluids, the eight radial dynamic fluid film coefficients are functions of both γ and ω , making a closed form solution to the simultaneous Eqs. (11) and (12) impossible and the solution is most conveniently obtained graphically. For any fixed value of ω , Δ_c and Δ_s can be plotted as functions of γ to find their zero points. With $\gamma > 0$ it is seen that Δ_s has one zero point and Δ_c has up to two zero points (only true in this simple case). The calculation is repeated for several values of ω and the results for the various zero points may be plotted as shown:

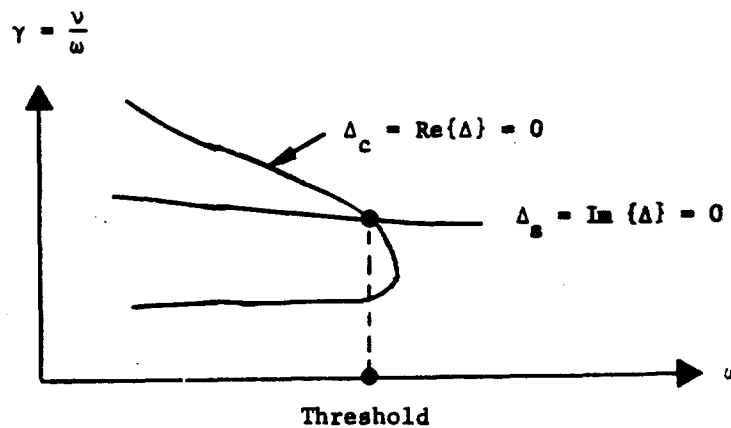


Fig. 2 Loci of Roots for Real and Imaginary Parts of Eq. (10)

The intersection of the two curves define the speed at which instability sets in or the point at which both the real and imaginary parts of the simplified determinant vanish simultaneously.

2. Analysis of Stability of Arbitrary, Non-Symmetrical Rotor

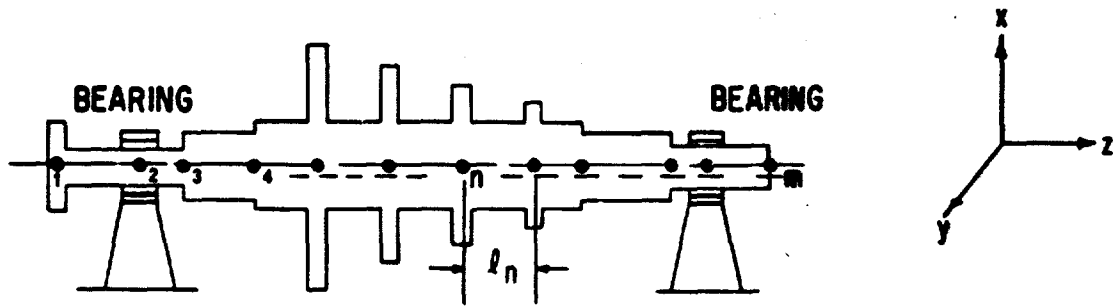
Consider the arbitrary rotor shown in Fig. 3. Assuming that the two ends of the rotor are free, the bending moments M'_{xm} and M'_{ym} and shear forces V'_{xm} and V'_{ym} at the rotor end will be linearly proportional to the displacements x_1 and y_1 and bending angles θ_1 and ϕ_1 of the shaft at station 1 provided these displacements and bending angles are small enough such that linearized analysis applies. Mathematically we can write this linear relationship as

$$\begin{pmatrix} V'_{xm} \\ V'_{ym} \\ M'_{xm} \\ M'_{ym} \end{pmatrix} = \begin{pmatrix} a_{11} & a_{12} & a_{13} & a_{14} \\ a_{21} & a_{22} & a_{23} & a_{24} \\ a_{31} & a_{32} & a_{33} & a_{34} \\ a_{41} & a_{42} & a_{43} & a_{44} \end{pmatrix} \begin{pmatrix} x_1 \\ y_1 \\ \theta_1 \\ \phi_1 \end{pmatrix} \quad (15)$$

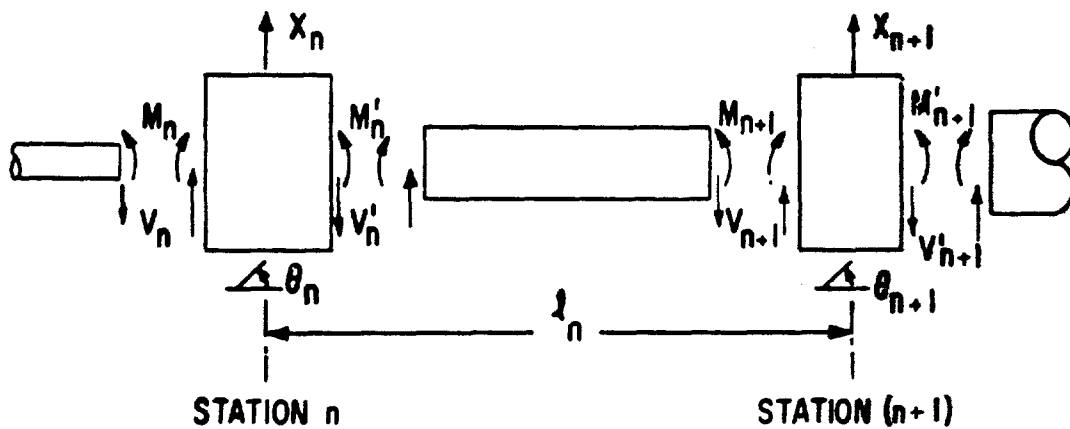
where the terms a_{11} , a_{12} , etc., are the dynamic influence coefficients which relate the forces at station m to the motions at station 1. These coefficients are functions of the rotor inertia, rotor flexibility, and the dynamic stiffness and damping coefficients of the bearings supporting the rotor. Since a_{11} , a_{12} , etc., are dynamic coefficients, they explicitly depend upon the rotor speed ω and the frequency ratio $\gamma = \nu/\omega$ where ν is the frequency of the shaft motions being considered. For gas bearing, the stiffness and damping coefficients contained in a_{11} , a_{12} , etc., are also functions of ω and γ .

For symmetrical, rigid rotors for which only translatory motions x_1 and y_1 are considered, Eq. (15) above reduces to

$$\begin{pmatrix} V'_{xm} \\ V'_{ym} \end{pmatrix} = \begin{pmatrix} a_{11} & a_{12} \\ a_{21} & a_{22} \end{pmatrix} \begin{pmatrix} x_1 \\ y_1 \end{pmatrix} \quad (16)$$



Outline of Rotor with Location of Rotor Stations



Sign Convention for Amplitude, Slope, Bending Moment and Shear Force illustrated in x-z Plane

Fig. 3

This is the situation considered in the previous section, and we see by comparison of Eq. (15) with Eq. (8) that the coefficients a_{11} , a_{12} , a_{21} , and a_{22} are given by the analytical expressions

$$\begin{aligned} a_{11} &= (Z_{xx} - Mv^2) \\ a_{12} &= Z_{xy} \\ a_{21} &= Z_{yx} \\ a_{22} &= (Z_{yy} - Mv^2) \end{aligned} \tag{17}$$

For the more general case of an arbitrary flexible rotor supported on dissimilar bearings, the coefficients a_{11} , a_{12} , etc., are very complex functions and usually cannot be expressed in analytical form but must be calculated by means of a computer program. Therefore, one of the principal tasks to be performed by a computer program written for analyzing the stability of arbitrary rotors is that of calculating all of the dynamic influence coefficients as a function of rotor geometry, rotor speed, frequency ratio γ and the dynamic bearing coefficients supplied as input to the program. The procedure by which these influence coefficients are calculated is described in Ref. 3, Appendix VIII.

Once the dynamic influence coefficients are calculated for an appropriate range of ω and γ , the various thresholds of stability of the rotor-bearing system are determined by essentially the same procedure as for the simple, symmetrical rotor-bearing system discussed in the previous section. That is, thresholds of instability are found by determining the values of ω and γ at which both the real and the imaginary parts of the determinant of the matrix of dynamic influence coefficients simultaneously go to zero. Again, this is accomplished by plotting on a graph of γ versus ω separate curves for the conditions where the real and the imaginary parts of the determinant go to zero, and determining the thresholds of instability from the intersections of these curves.

In the case of an arbitrary rotor which is flexible and unsymmetric, determining

the real and imaginary parts of the determinant of the matrix of influence coefficients cannot, in general, be accomplished analytically but must be accomplished numerically by the computer program for analyzing stability. The procedure is essentially one of having the computer program calculate the values of the real and imaginary parts of the determinant over a specified range of whirl frequency ratios at a fixed rotor speed. The program then determines the zero points of the real and imaginary parts of the determinant by quadratic interpolation each time a change in the sign of these functions occurs. It should be clearly noted here that the computer program itself does not determine thresholds of stability; this remains to be accomplished by the designer by plotting the curves of the loci of the real and imaginary roots of the stability determinant.

The discussion presented above serves to describe in a qualitative way the nature of the process of determining the stability of an arbitrary rotor and how this process is implemented by means of a computer program. A detailed description of the computer program developed in the present project for the purpose of analyzing rotor-bearing stability is given in Appendix I.

3. Determination of Rotor-Bearing Stability by Means of Critical Speed Maps.

For a flexible rotor with two translatory and two angular degrees of freedom, i.e., x_1 , y_1 , θ_1 and ω_1 the determinant of the matrix of influence coefficients is a higher order polynomial in γ and ω than is the simple determinant from Eq. (9). Consequently, there are many real and imaginary roots of the determinant and a number of different thresholds of instability, i.e., a plot such as that shown in Fig. 2 will, for an arbitrary flexible rotor, contain many curves for $\Delta_c = 0$ and $\Delta_s = 0$ and many curve intersections. Each different intersection or threshold of stability will correspond to a different mode of instability motion, e.g., translatory whirl, conical whirl, etc. In general, only the mode occurring at the lowest value of ω is of interest since this defines the practical operating limits of the system. However, the presence of a number of modes of instability makes the determination of the lowest mode a very complex and costly task, even with the aid of the computer program. Hence, it is desirable to find methods of approximately determining thresholds of instability so that the exact process of determinin

such thresholds by means of the stability program can be accomplished with a minimum of costly searching.

One convenient approach for approximately locating the instabilities of most rotors can be had by use of a critical speed map for the rotor in question. A critical speed map shows the various natural or resonant frequencies of a rotor as a function of a single value of spring stiffness K assigned to the bearings supporting the shaft. A typical critical speed map is shown in Fig. 10. For complex rotors, such maps are usually obtained by means of a computer program written specifically for this purpose.

As was discussed earlier in subsection 1., whirl instability can be viewed as a condition of undamped resonance. In particular Lund (Ref. 4) has shown that if this view point is taken, then at the threshold of stability the fluid film bearing can be represented by a single effective spring stiffness coefficient K and damping coefficient B given by

$$K = \frac{1}{2}(K_{xx} + K_{yy}) - \frac{\frac{1}{4}(K_{xx} - K_{yy})(\gamma_{\omega B_{xx}} - \gamma_{\omega B_{yy}}) + \frac{1}{2}(K_{xy} \gamma_{\omega B_{yx}} + K_{yx} \gamma_{\omega B_{xy}})}{A} \quad (18)$$

$$B = \frac{1}{2}(\gamma_{\omega B_{xx}} + \gamma_{\omega B_{yy}}) - A \quad (19)$$

where A is expressed by the following quartic equation:

$$A^4 + \left[\frac{1}{4} (K_{xx} - K_{yy})^2 + K_{xy} K_{yx} - \frac{1}{4} (\gamma_{\omega B_{xx}} - \gamma_{\omega B_{yy}})^2 - \gamma_{\omega B_{xy}} \gamma_{\omega B_{yx}} \right] A^2 - \left[\frac{1}{4} (K_{xx} - K_{yy})(\gamma_{\omega B_{xx}} - \gamma_{\omega B_{yy}}) + \frac{1}{2} (K_{xy} \gamma_{\omega B_{yx}} + K_{yx} \gamma_{\omega B_{xy}}) \right]^2 = 0 \quad (20)$$

Since B is real, Eq. (20) has only two solutions for A which are of equal magnitude but of opposite sign. In order for the effective bearing damping to become zero (corresponding to the undamped resonance criteria) at some value of γ , then A must be positive from Eq. (20) since $(\gamma_{DB_{xx}} + \gamma_{DB_{yy}})$ is always positive. Therefore, only the real, positive value of A is used to define the stiffness coefficient in Eq. (18).

Another method of obtaining the effective stiffness and damping bearing coefficients at the threshold of stability is by replacing Mv^2 by Z in Eq. (9) and then solving for Z. From Eq. (9):

$$\begin{Bmatrix} (Z_{xx} - Z) & Z_{xy} \\ Z_{yx} & (Z_{yy} - Z) \end{Bmatrix} \begin{Bmatrix} x \\ y \end{Bmatrix} = 0 \quad (21)$$

Since two solutions of Z are obtained, the following notation is used:

$$Z_1, Z_2 = \begin{Bmatrix} Z_{\text{major}} \\ Z_{\text{minor}} \end{Bmatrix} = \frac{1}{2} \left[(Z_{xx} + Z_{yy}) \pm \sqrt{(Z_{xx} - Z_{yy})^2 + 4Z_{xy} Z_{yx}} \right] \quad (22)$$

where:

$$Z_{xx} = K_{xx} + i\gamma_{DB_{xx}} \quad (\text{Similarly for } Z_{xy}, Z_{yx}, Z_{yy})$$

$$Z_{\text{major}} = K_{\text{major}} + i\gamma_{DB_{\text{major}}} \quad (\text{Similarly for } Z_{\text{minor}})$$

The condition for the lowest threshold speed is that $\gamma_{DB_{\text{minor}}} = 0$. Thus the K_{minor} and B_{minor} are equivalent to the two expressions shown in Eqs. (18) and (19).

In arriving at a K_{minor} and a B_{minor} value, the negative sign in front of the radical in Eq. (22) is generally used. An evaluation of the value of the radical is somewhat difficult since the coefficients of the bearing change constantly with increasing eccentricity. Various bearing types and coefficients have been evaluated and this sign convention has proven correct. This sign convention is also consistent with the analysis by Lund (Ref. 4).

The importance of K_{minor} lies in the convenience with which it can be used in conjunction with a rotor critical speed map to determine the onset of instability. By cross-plotting the minor stiffness of the bearing as a function of rotor speed, several critical speed curves may be crossed before the rotor design speed is reached. The threshold speed is obtained when the first critical speed corresponding to K_{minor} , divided by the critical whirl frequency ratio γ , gives the rotor speed at which the K_{minor} and γ were evaluated. The critical whirl frequency ratio is defined as the value of v/ω at which B evaluated from Equation (19) goes to zero. In most instances, the critical frequency ratio is nearly 1/2, and since K_{minor} tends not to change very rapidly with rotor speed, this gives rise to the rule of thumb that the whirl threshold speed is approximately twice the first critical speed of the rotor bearing system. The critical whirl frequency ratio can be determined from Eq. (14).

The specific steps involved in determining threshold speed from a critical speed map are as follows:

- (1) Obtain a critical speed map of the rotor as a function of support stiffness.
- (2) Calculate the eight radial bearing coefficients over some specified speed range which one estimates will contain the whirl threshold speed.
- (3) Compute the K_{minor} and γ values from Eqs. (18) or (22) and (14), for various shaft speeds.

- (4) For each of the K_{minor} values, enter the critical speed map at each value and obtain the first natural frequency or critical speed.
- (5) For each shaft speed selected divide the critical speed by the computed whirl frequency ratio. When the resulting speed, which we shall refer to as apparent threshold speed, equals the shaft speed at which the K_{minor} value was evaluated, then the actual threshold speed has been determined.

For incompressible lubricated bearings the stiffness and damping coefficients are independent of the whirl frequency ratio, whereas the compressible lubricated bearing coefficients must be obtained at the critical whirl frequency ratio. In general these gas bearing coefficients may be obtained at $v/\omega = 0.50$ with sufficient accuracy since the critical whirl frequency ratio is usually close to this value.

It should be noted that use of a critical speed map together with values of K_{minor} to determine the stability threshold is valid for rotors of arbitrary shape and flexibility but does rely upon the bearings supporting the rotor being quite similar, since the critical speed map is plotted in terms of only one value of bearing stiffness. However, if the bearings supporting the rotor are not too dissimilar, the present approach will serve to indicate at least approximately the critical speed and critical speed ratio by using values of K_{minor} for any one of the bearings. A more exact value for critical speed can then be determined by using the computer program developed for calculating rotor bearing stability.

An example calculation of how to determine whirl threshold speed from a critical speed map is given in the next section.

SECTION III

EFFECT OF THRUST BEARING STIFFNESS AND DAMPING ON ROTOR-BEARING STABILITY

1. Discussion

Since a thrust bearing exhibits no radial stiffness or radial damping properties, the threshold speed of a rotor which whirls in the lateral or radial mode will not be affected. However, if the rotor motion is angular or conical, considerable restraint can be imposed on the rotor by the angular thrust bearing properties. Thus, if the lowest critical speed of the rotor is conical, the threshold speed of the rotor could be significantly influenced by the addition of the thrust bearing coefficients. The computer program described in Appendix I of this report allows for the inclusion of these thrust bearing coefficients. In this present section we will consider some simplified relations which enable us to estimate the effects of thrust bearing stiffness on the conical stability of a symmetric rotor.

First let us define the axes about which the rotor undergoes angular displacement while whirling in a conical mode. Consider Fig. 4. The two coordinates which serve to define the angular displacement of each thrust bearing are the θ coordinate, which measures rotation about the y axis and the φ coordinate which measures rotation about the x axis. Both of these coordinates are shown about point O at the center of the rotor bearing system. These angular rotations are defined by $\tan \theta = dx/dz^*$ and $\tan \varphi = dy/dz^*$. The equations defining the angular dynamic coefficients are:

$$M_x = -G_{xx} \theta - D_{xx} \frac{d\theta}{dt} - G_{xy} \varphi - D_{xy} \frac{d\varphi}{dt} \quad (23)$$

$$M_y = -G_{xy} \theta - D_{yx} \frac{d\theta}{dt} - G_{yy} \varphi - D_{yy} \frac{d\varphi}{dt} \quad (24)$$

where M_x and M_y are the dynamic moments acting on the rotor resulting from the angular displacements and velocities $\theta, \varphi, d\theta/dt$ and $d\varphi/dt$. M_x is in the x-z plane while M_y is in the y-z plane.

* For a flexible rotor, local values of dx/dz and dy/dz serve to define the angular rotations θ and φ at local points along the rotor.

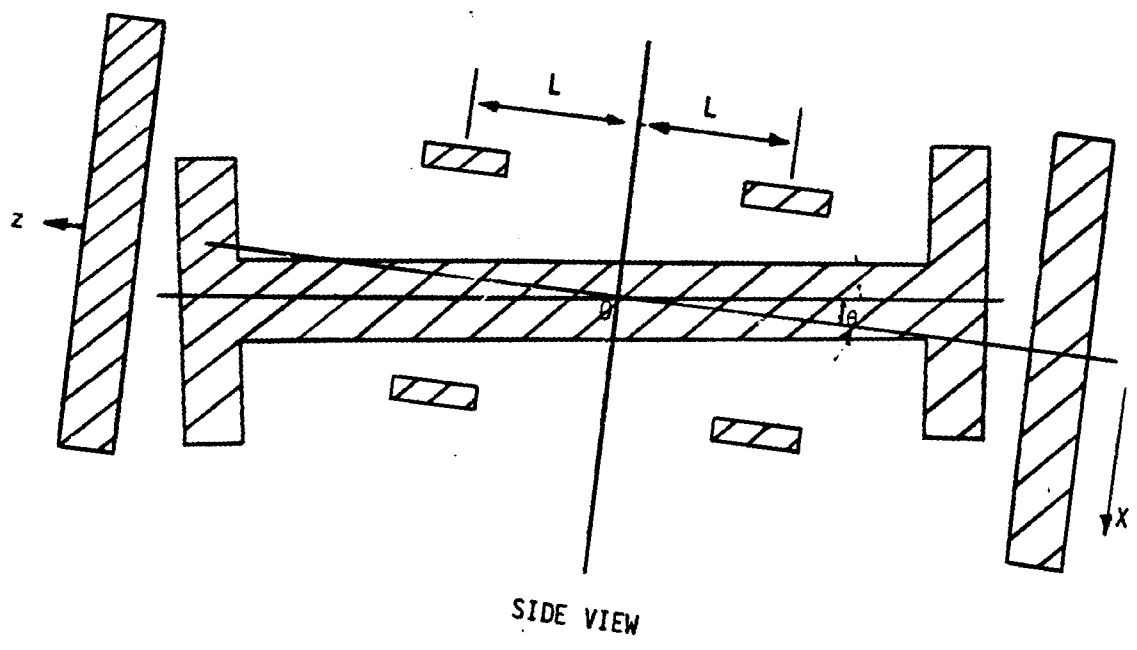
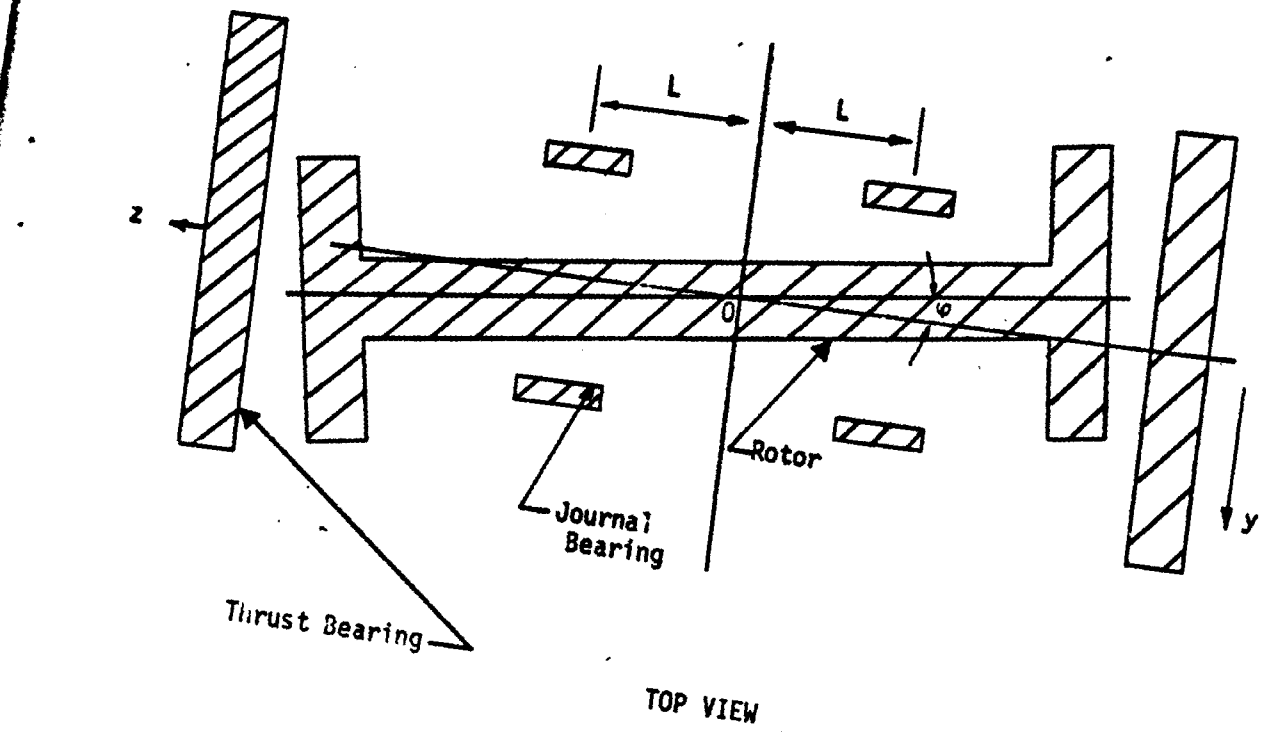


Fig. 4 Coordinate Axis System

The computer program written to analyze rotor-bearing stability accepts the eight angular stiffness and damping coefficients G_{xx} , ωD_{xx} , G_{xy} , etc., directly as bearing input data along with the translatory coefficients K_{xx} , ωB_{xx} , K_{xy} , etc. However, in order to gain an estimate of the effect of thrust bearing angular stiffness on rotor-bearing stability, it is convenient to try to use the critical speed map approach for determining whirl-instability that was described earlier in the report. To use this approach, it is necessary to relate the thrust bearing angular coefficients to effective translatory stiffness and damping coefficients of the journal bearings supporting the rotor. For a symmetrical rotor-bearing system this can be accomplished by the following geometrical considerations. Referring to Fig. 4 we see that the restoring moment $(M_x)_j$ in the x-z plane exerted by each journal bearing in response to a static angular displacement θ about an axis through the point 0 parallel to the θ axis is

$$(M_x)_j = -K_{xx} L^2 \theta \quad (25)$$

Similarly, the restoring moment $(M_y)_j$, due to each journal bearing is

$$(M_y)_j = -K_{yx} L^2 \theta \quad (26)$$

On the other hand, the restoring moments $(M_x)_T$ and $(M_y)_T$ exerted by each thrust bearing due to the angular displacement θ are given by Eqs. (23) and (24), i.e.,

$$(M_x)_T = -G_{xx} \theta \quad (27)$$

$$(M_y)_T = -G_{yx} \theta \quad (28)$$

Therefore, we see that for angular displacement in this symmetrical system, the restoring moments of thrust bearings can be represented simply by adding the "effective" stiffness coefficients G_{xx}/L^2 and G_{yx}/L^2 respectively to the existing coefficients K_{xx} and K_{yx} of the journal bearings. This applies as well to all of the stiffness and damping coefficients. This, for angular displacements about axes through the point 0, the restoring moments can be determined by assuming that each journal bearing has effective stiffness and damping coefficients $(K_{xx})_e$.

$(B_{xx})_e, (K_{xy})_e, \text{etc.},$ given by

$$(K_{xx})_e = K_{xx} + G_{xx}/L^2$$

$$(K_{xy})_e = K_{xy} + G_{xy}/L^2$$

$$(K_{yx})_e = K_{yx} + G_{yx}/L^2$$

$$(K_{yy})_e = K_{yy} + G_{yy}/L^2$$

$$(B_{xx})_e = B_{xx} + D_{xx}/L^2$$

$$(B_{xy})_e = B_{xy} + D_{xy}/L^2$$

$$(B_{yx})_e = B_{yx} + D_{yx}/L^2$$

$$(B_{yy})_e = B_{yy} + D_{yy}/L^2$$

(29)

The approach of taking account of thrust bearing effects on conical motions of symmetrical systems by means of adding effective stiffness and damping to existing journal bearings permits one to use the critical speed map method for estimating whirl instability as described in the previous section. This would be accomplished by using the total effective values of stiffness for conical motion of the rotor, as defined in Eqs. (29) to evaluate K_{minor} and overall damping B as defined by Eqs. (18), (19) and (20). Note that this procedure is valid for conical whirl instability only. Thrust bearings would have no effect on the translatory whirl mode and their angular coefficients should not be included in the evaluation of K_{minor} and B if this mode of instability is being determined.

Some sample calculations were performed by the critical speed map method to examine the effect of independently adding principal angular stiffness, G_{xx} and G_{yy} and principal angular damping D_{xx} and D_{yy} on the conical stability of a symmetrical rotor. The conclusions reached were that:

- (1) Addition of principal angular stiffnesses G_{xx} and G_{yy} does not change the critical value of frequency ratio γ_c for instability but can increase the threshold speed ω_c for instability by increasing the natural frequency of the conical mode.
- (2) Addition of principal angular damping, D_{xx} and D_{yy} , does not change the natural frequency of the rotor-bearing system, but does decrease the critical frequency ratio for instability (i.e., the frequency ratio at which damping B goes to zero) thereby increasing the threshold speed ω_c at which instability occurs.

In the sub-section below are discussed various specific design examples for which the effect of thrust bearings on rotor-bearing stability are investigated.

2. Sample Calculations

The basic tool used in computing the threshold speed is computer program PN400. With this program it was possible to obtain the threshold speeds exactly with and without the thrust bearing effects. However, since much time searching for threshold speeds is generally required when using this program alone, the shorter critical speed map technique for locating threshold speeds, outlined in this report, was first used to obtain an approximate value of threshold speed with an exact solution being then obtained using the computer program.

Two rotors will be analyzed to determine their threshold speeds with and without the addition of a thrust bearing system. These two rotor models are shown in Figures 5 and 6.

The first rotor, Figure 5, weighs approximately 7.2 lbs. and is supported by two gas-lubricated hydrodynamic journal bearings. The load is identical on each bearing. Air at 100°F and ambient pressure (14.7 psia) is supplied to each bearing. Thrust bearing surfaces are available at either end of the rotor.

The second rotor, Figure 6, weighs approximately 18.75 lbs. and is supported by

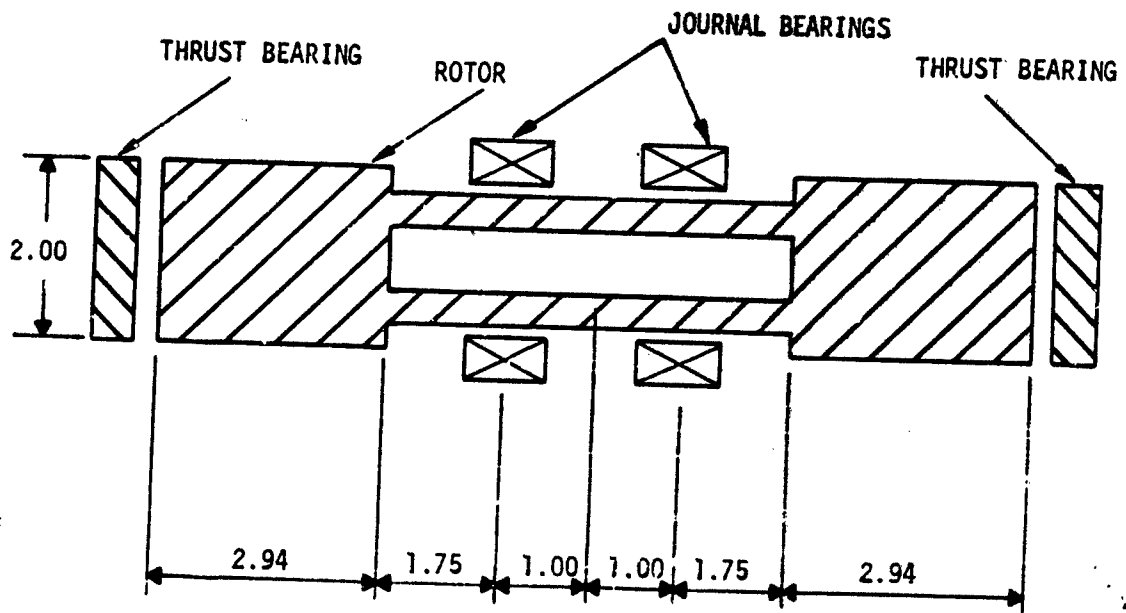


Fig. 5 Conical Instability Rotor Model 1

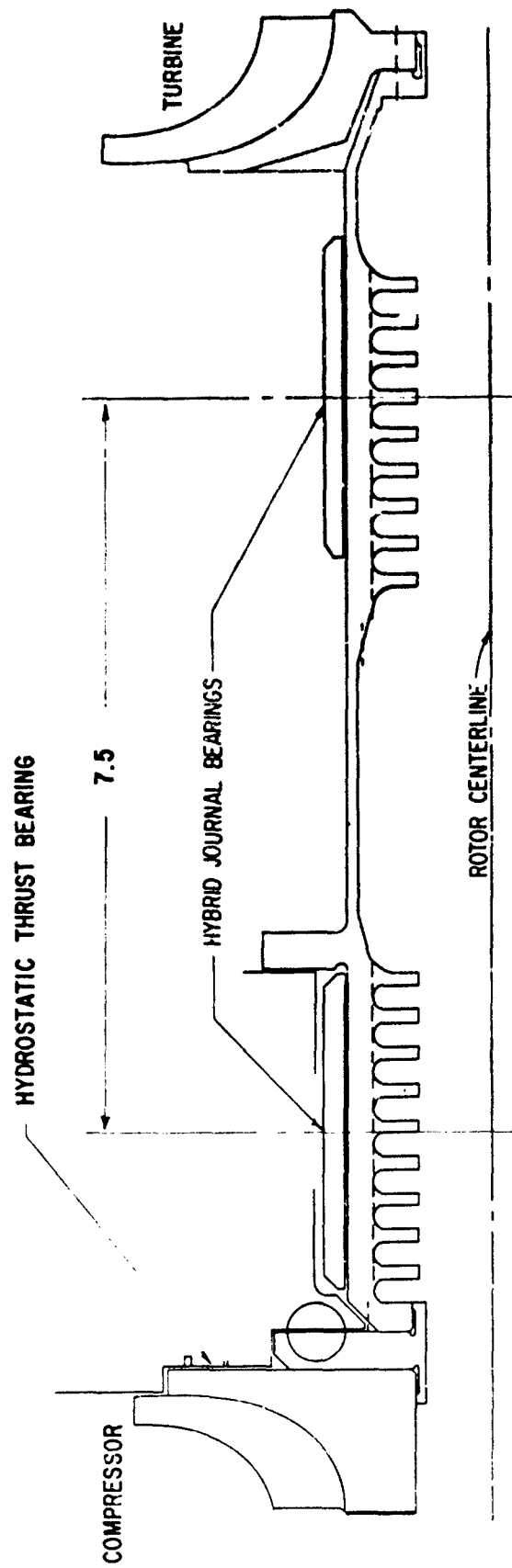


Fig. 6 Conical Instability Rotor Model 2

two gas-lubricated hybrid journal bearings. The loads are different for each bearing. A thrust bearing is shown at the left hand end of the rotor. This particular model was designed as a high pressure (HP) spool for an actual high temperature turbo-compressor but the design was rejected based on its threshold speed. No consideration was given to the thrust bearing effects on the rotors' stability behavior. In this example the thrust bearing effects will be computed.

Tables I and II list the nondimensional dynamic coefficients for the hydrodynamic and hybrid gas-lubricated journal bearing designs respectively. Table I lists the eight stiffness and damping coefficients as a function of eccentricity (or load), bearing number Λ and whirl frequency ratio v/ω for a length-to-diameter ratio of 1.00. For a constant load on a bearing (\bar{W} constant) and varying speed the coefficients must be obtained by double interpolation on Λ and load in Table I since Λ changes with speed. Although data are shown for $v/\omega = 0.3, 0.5$ and 1.00, only the $v/\omega = 0.5$ data was used in the first example.

The data for rotor No. 1 are given below

Rotor Model #1

Journal Bearing Design (Hydrodynamic)

D = 1.50 in.
L = 1.50 in.
C/R = .001 in/in.
P_a = 14.7 psia
W = 3.62 lbs. (each bearing)
 $\mu = 2.7 \times 10^{-9}$ lb.sec/in² (air at 100°F)

Thrust Bearing Design (Hydrostatic)

R_o = 1.00 in.
R_i = 0.333 in.
P_a = 14.7 psia
P_s = 73.5
C = .0011 in.
Inherent compensation
 $\Lambda_s = 1.0$

TABLE I
FLAIN CYLINDRICAL BEAKING
COMPRESSIBLE DATA

$L/D = 1$

ν/ω	λ	$\epsilon_B \cos \phi_B$	ϵ_B	ϕ_B	\bar{W}	\bar{K}_{xx}	\bar{K}_{xy}	\bar{K}_{yx}	\bar{K}_{yy}	\bar{B}_{xx}	\bar{B}_{xy}	\bar{B}_{yx}	\bar{B}_{yy}
0.3	0.50	.075	.375	78.5	.052	1.54	3.49	- 3.10	1.78	4.98	- 1.30	3.30	8.50
		.10	.43	76.5	.063	1.55	3.30	- 2.50	1.90	4.30	- 1.10	3.30	7.60
		.15	.51	73.0	.090	1.53	3.20	- 1.03	2.10	3.50	- 1.00	3.28	6.26
		.20	.57	69.4	.110	1.69	3.22	- 1.16	2.32	3.16	- .86	3.38	5.47
1.00		.075	.27	73.8	.067	2.27	3.85	- 3.90	2.56	5.87	- 3.37	5.30	8.70
		.10	.32	71.7	.083	2.10	3.40	- 3.00	2.50	4.80	- 2.83	4.70	7.00
		.15	.40	68.0	.12	1.94	2.96	- 1.90	2.42	3.72	- 2.24	3.98	5.11
		.20	.46	64.3	.15	2.00	2.78	- 1.27	2.48	3.17	- 1.90	3.64	4.02
1.60		.006	.006		.007	123.	43.0	-140.	140.	-207.	-117.	267.	7.17
		.011	.011		.014	61.6	21.4	- 70.	70.6	-104.	- 58.6	132.	3.40
		.028	.028		.035	25.0	8.54	- 27.5	28.4	- 41.4	- 23.5	51.6	1.15
		.055	.055		.072	12.8	4.26	- 13.4	14.3	- 20.6	- 11.8	24.7	.41
1.80		.006	.006		.007	127.	40.8	-144.	145.	-222.	-110.	268.	5.44
		.011	.011		.014	63.7	20.4	- 71.8	72.7	-111.	- 55.0	133.	2.56
		.027	.027		.036	25.8	8.14	- 28.2	29.2	- 44.0	- 22.0	51.8	.839
		.055	.055		.072	13.2	4.05	- 13.7	14.7	- 22.0	- 11.1	24.8	.280
2.00		.075	.18	65.4	.080	3.70	4.20	- 5.00	4.00	5.30	- 7.20	9.00	8.30
		.10	.22	63.6	.10	3.20	3.50	- 3.60	3.40	4.20	- 5.70	7.00	6.10
		.15	.30	60.0	.15	2.63	2.76	- 2.20	2.88	3.11	- 4.10	5.00	3.82
		.20	.36	56.5	.19	2.48	2.41	- 1.43	2.67	2.51	- 3.27	4.00	2.65

TABLE I (Continued)
 PLAIN CYLINDRICAL BEARING
 COMPRESSIBLE DATA

$$L/D = 1$$

v/ω	Λ	$\epsilon_B \cos \phi_B$	ϵ_B	ϕ_B	\bar{W}	\bar{K}_{xx}	\bar{K}_{xy}	\bar{K}_{yx}	\bar{K}_{yy}	\bar{B}_{xx}	\bar{B}_{xy}	\bar{B}_{yx}	\bar{B}_{yy}
0.3	4.00	.005	.009	55.0	.007	67.2	57.1	-98.0	77.5	7.50	-155.	218.	93.0
		.01	.017	54.8	.014	34.0	28.7	-48.6	39.0	3.88	-78.0	109.	46.0
		.025	.043	54.1	.034	14.3	11.7	-19.1	16.0	1.71	-31.7	42.8	17.9
		.05	.083	52.9	.067	7.70	5.10	-9.30	8.40	1.00	-1.61	20.8	8.44
		.075	.12	52.3	.088	5.60	4.00	-6.00	5.80	7.00	-11.0	13.2	5.70
		.10	.16	51.0	.12	4.50	3.20	-4.30	4.60	6.10	-8.40	9.60	4.00
		.15	.22	48.0	.18	3.47	2.39	-2.57	3.46	6.36	-5.70	6.13	2.22
		.20	.284	45.2	.236	3.03	1.95	-1.69	2.96	0.55	-4.40	4.30	1.40
		.005	.007	45.7	.007	84.5	55.2	-109.	98.4	-56.7	-163.	251.	57.4
		.01	.014	45.5	.014	42.7	27.7	-54.2	49.4	-28.3	-82.0	124.	28.3
.50	6.00	.025	.035	44.9	.034	17.6	11.2	-21.3	20.0	-11.2	-33.0	48.7	10.8
		.05	.069	43.8	.068	9.33	5.70	-10.3	10.3	-5.50	-16.8	23.4	4.97
		.075	.10	43.7	.09	6.60	3.70	-6.70	6.90	-3.70	-11.7	14.6	3.70
		.10	.14	42.5	.12	5.30	2.90	-4.80	5.30	-2.70	-8.90	10.5	2.50
		.15	.196	40.0	.190	3.90	2.11	-2.90	3.84	-1.57	-5.90	6.57	1.50
		.20	.253	37.7	.256	3.30	1.67	-1.94	3.10	-1.12	-4.50	4.48	0.79
		.005	.058	85.0	.008	4.80	16.4	-22.6	5.57	33.1	-8.45	11.4	46.9
		.010	.10	84.5	.014	3.06	9.34	-12.4	3.45	18.3	-4.64	6.65	26.2
		.025	.20	82.9	.028	2.03	5.13	-6.06	2.35	9.32	-2.38	3.91	13.8
		.050	.30	80.6	.046	1.71	3.77	-3.66	2.17	6.06	-1.61	3.14	9.56

TABLE I (Continued)
PLAIN CYLINDRICAL BEARING
COMPRESSIBLE DATA

$\frac{L}{D} = 1$

v/w	Λ	$e_B \cos \phi_B$	e_B	ϕ_B	\bar{w}	\bar{K}_{xx}	\bar{K}_{xy}	\bar{K}_{yz}	\bar{K}_{yy}	\bar{B}_{xx}	\bar{B}_{xy}	\bar{B}_{yx}	\bar{B}_{yy}
.50	.50	.075	.375	78.5	.052	1.77	3.41	-2.77	2.30	4.89	-1.28	3.10	8.30
		.10	.43	76.5	.063	1.75	3.20	-2.20	2.40	4.20	-1.10	3.00	7.30
		.15	.51	73.0	.090	1.71	3.12	-1.25	2.55	3.45	-0.97	3.00	6.00
		.20	.57	69.4	.110	1.87	3.16	-0.69	2.75	3.10	-0.82	3.07	5.22
		.005	.04	83.0	.007	8.16	21.8	-30.4	9.86	44.2	-15.2	20.0	62.9
	.67	.01	.078	82.6	.014	4.74	11.8	-15.9	5.57	23.4	-8.05	10.9	33.4
		.025	.16	81.2	.03	2.75	5.87	-7.19	3.21	11.0	-3.82	5.57	15.9
		.05	.26	78.9	.05	2.12	3.99	-4.08	2.63	6.75	-2.43	3.98	10.1
		.075	.33	76.8	.067	1.94	3.40	-2.89	2.55	5.24	-1.95	3.52	8.03
		.005	.027	79.3	.007	16.2	29.7	-42.5	20.4	60.4	-31.5	40.8	87.7
1.00	.01	.052	.052	79.0	.014	8.76	15.4	-21.5	10.8	31.0	-16.2	21.0	45.0
		.025	.12	77.8	.03	4.36	7.00	-9.00	5.20	13.5	-7.10	9.43	19.4
		.050	.20	75.8	.056	2.96	4.39	-4.70	3.59	7.68	-4.13	5.74	11.0
		.075	.27	73.8	.067	2.66	3.48	-3.20	3.23	5.70	-3.10	4.70	8.4
		.10	.32	71.7	.083	2.47	3.10	-2.40	3.00	4.70	-2.6	4.00	6.8
	.15	.40	.40	68.0	.12	2.20	2.70	-1.32	2.83	3.62	-2.06	3.38	4.89
		.46	.46	64.3	.15	2.22	2.56	-0.72	3.80	3.07	-1.74	3.03	3.87
		.006	.006		.007	48.8	9.34	-26.7	146.	35.0	-96.0	286.	69.4
		.011	.011		.014	24.9	4.64	-13.3	73.0	17.3	-47.8	142.	34.6
		.028	.028		.035	10.5	1.82	-5.24	29.3	6.73	-19.0	56.0	13.8

TABLE I (Continued)
 PLAIN CYLINDRICAL BEARING
 COMPRESSIBLE DATA

$$\frac{L}{D} = 1$$

ν/ω	Λ	$\epsilon_B \cos \phi_B$	ϵ_B	ϕ_B	\bar{W}	\bar{K}_{xx}	\bar{K}_{xy}	\bar{K}_{yx}	\bar{K}_{yy}	\bar{B}_{xx}	\bar{B}_{xy}	\bar{B}_{yx}	\bar{B}_{yy}
.50	1.60		.055		.072	5.76	0.89	-2.50	14.8	3.20	-9.40	27.2	6.80
	2.00	.005	.014	69.4	.007	38.6	35.8	-5.70	52.0	74.4	-76.5	103.	119.
4.00		.01	.028	69.2	.013	20.0	18.2	-28.4	26.4	37.5	-38.7	51.8	59.5
		.025	.068	68.3	.033	8.75	7.69	-11.2	11.1	15.4	-16.0	21.0	24.0
		.05	.13	66.7	.063	5.10	4.24	-5.49	6.20	8.00	-8.47	10.7	12.2
		.075	.18	65.4	.08	4.00	3.10	-3.60	4.70	5.50	-5.90	7.30	8.40
		.10	.22	63.6	.10	3.50	2.60	-2.50	3.90	4.30	-4.70	5.70	6.40
		.15	.30	60.0	.15	2.84	2.10	-1.37	3.16	3.17	-3.37	3.95	4.10
		.20	.36	56.5	.19	2.66	1.88	-.76	2.82	2.54	-2.70	3.08	3.00
		.005	.009	55.0	.007	56.7	26.7	-54.0	89.0	59.4	-113.	175.	116.
		.01	.017	54.9	.013	29.0	13.5	-27.0	44.7	30.0	-56.6	87.4	57.8
		.025	.043	54.1	.034	12.2	5.52	-10.6	18.2	11.8	-23.0	34.0	23.0
6.00		.05	.083	52.9	.067	6.72	2.90	-5.14	9.40	5.90	-11.7	16.9	11.4
		.075	.12	52.3	.088	5.00	1.90	-3.40	6.50	3.70	-7.90	10.7	8.00
		.10	.16	51.0	.12	4.10	1.50	-2.40	5.00	2.80	-6.00	7.90	5.90
		.15	.22	48.0	.18	3.22	1.25	-1.35	3.67	2.06	-4.14	5.02	3.62
		.20	.284	45.2	.236	2.87	1.10	-.83	3.00	1.55	-3.17	3.56	2.59
		.005	.007	45.7	.007	59.4	19.5	-47.0	108.	47.6	-118.	212.	104.
		.01	.014	45.5	.014	30.0	9.80	-23.5	54.0	23.7	-59.0	105.	52.0
		.025	.035	44.9	.034	12.7	3.96	-9.30	21.8	9.93	-23.7	41.5	20.7

TABLE I (Continued)
PLAIN CYLINDRICAL BEARING
COMPRESSIBLE DATA

$L/D = 1$

ν/ω	Λ	$\epsilon_B \cos \phi_B$	ϵ_B	ϕ_B	\bar{W}	\bar{K}_{xx}	\bar{K}_{xy}	\bar{K}_{yx}	\bar{K}_{yy}	\bar{B}_{xx}	\bar{B}_{xy}	\bar{B}_{yx}	\bar{B}_{yy}
.50	6.00	.05	.069	43.8	.068	6.90	2.00	- 4.50	11.0	4.60	-12.0	20.0	10.2
		.075	.10	43.7	.09	5.10	1.20	- 3.20	7.50	2.50	- 8.00	12.8	7.50
		.10	.14	42.5	.12	4.20	.93	- 2.30	5.80	1.90	- 6.00	9.30	5.50
		.15	.20	40.0	.19	3.20	.82	- 1.24	4.07	1.50	- 4.10	5.84	3.33
		.20	.25	37.7	.26	2.80	.69	- .80	3.24	1.07	- 3.07	4.10	2.40
1.00	0.50	.15	.51	73.0	.090	2.47	2.83	- .03	4.26	3.19	- .84	2.10	5.10
		.20	.57	69.4	.11	2.60	2.91	.59	4.28	2.82	- .70	2.04	4.34
		.005	.03	80.4	.007	27.2	17.7	-26.6	40.2	51.1	-19.8	26.1	71.0
		.01	.058	80.0	.014	14.5	9.34	-13.4	21.0	26.4	-10.3	13.4	36.6
		.025	.13	78.8	.031	7.01	4.42	- 5.37	9.90	11.6	- 4.63	5.96	16.1
2.00	1.00	.05	.22	76.7	.054	4.58	2.86	- 2.49	6.45	6.68	- 2.76	3.53	9.22
		.075	.28	74.6	.075	3.80	2.38	- 1.39	5.39	5.00	- 2.10	2.72	6.84
		.15	.40	68.0	.12	3.25	1.87	.069	4.37	3.13	- 1.43	1.80	4.05
		.20	.46	64.3	.15	3.15	1.86	.54	4.00	2.61	- 1.19	1.52	3.23
		.15	.30	60.0	.15	4.00	.69	.15	4.88	2.77	- 1.53	1.68	3.44
4.00	6.00	.20	.36	56.5	.13	3.59	.75	.39	4.10	2.16	- 1.20	1.25	2.63
		.15	.22	48.0	.18	4.69	-.05	.48	5.72	2.48	- 1.00	1.50	2.64
		.20	.284	45.2	.236	3.94	.089	.489	4.54	1.82	- .77	1.08	1.97
		.15	.196	40.0	.19	5.2	-.17	.63	6.10	2.30	- .70	1.24	2.10
		.20	.250	37.7	.256	4.24	-.03	.55	4.70	1.65	- .52	.88	1.55

TABLE II
 HYBRID BEARING DATA
 $L/D = 1.08, \nu/\omega = 0.50$

P_s/P_a	Λ_s	Λ	ϵ	\bar{W}	\bar{K}_{xx}	\bar{K}_{xy}	\bar{K}_{yx}	\bar{K}_{yy}	$\omega\bar{B}_{xx}$	$\omega\bar{B}_{xy}$	$\omega\bar{B}_{yx}$	$\omega\bar{B}_{yy}$
4.0	1.00	0.50	.01	.018	1.81	.0756	-.0756	1.81	.152	-.014	.014	.1510
			.02	.036	1.181	.0756	-.0757	1.81	.152	-.014	.014	.151
			.04	.0725	1.82	.0757	-.0757	1.815	.152	-.014	.014	.151
			.06	.109	1.83	.0757	-.0758	1.818	.152	-.014	.014	.152
			.08	.145	1.84	.0758	-.076	1.822	.152	-.014	.014	.152
	1.00	1.00	.01	.018	1.83	.148	-.147	1.83	.296	-.054	.054	.294
			.02	.0365	1.84	.148	-.148	1.83	.296	-.054	.054	.296
			.04	.073	1.84	.148	-.148	1.84	.296	-.054	.054	.296
			.06	.110	1.848	.148	-.148	1.838	.296	-.054	.054	.296
			.08	.147	1.860	.148	-.148	1.84	.296	-.054	.054	.296
	1.00	3.0	.01	.0197	2.00	.35	-.35	2.00	.70	-.386	.386	.70
			.02	.0394	2.00	.35	-.35	2.00	.70	-.386	.386	.70
			.04	.0789	2.00	.35	-.35	2.00	.70	-.386	.386	.70
			.06	.1185	2.02	.351	-.352	2.00	.704	-.388	.386	.70
			.08	.158	2.03	.351	-.353	2.00	.704	-.398	.386	.702
	1.00	5.00	.01	.022	2.186	.414	-.414	2.18	.828	-.758	.758	.828
			.02	.0438	2.187	.414	-.414	2.186	.828	-.758	.758	.828
			.04	.0876	2.193	.414	-.414	2.188	.828	-.758	.758	.828
			.06	.132	2.20	.414	-.415	2.19	.830	-.760	.758	.828
			.08	.176	2.22	.414	-.416	2.196	.832	-.762	.758	.828

Dimensionless Operating Parameters for Journal Bearings:

$$\begin{aligned} \Lambda &= \frac{12\pi\mu N}{P_a} \left(\frac{R_o}{C}\right)^2 \\ &= \frac{12\pi(2.7 \times 10^{-9})(N)}{14.7 (.001)^2} \\ &= 6.95 \times 10^{-3}(N) \text{ where } N = \text{speed, rps} \\ &= 1.16 \times 10^{-4}(N') \text{ where } N' = \text{speed, rpm} \\ \bar{W} &= \frac{W}{P_a LD} \\ &= \frac{3.62}{(14.7)(1.5)(1.5)} \\ &= 0.11 \end{aligned}$$

Values of journal bearing stiffness and damping coefficients were obtained from Table I for various pertinent values of Λ at $\nu/\omega = 0.5$ for $\bar{W} = 0.11$. Corresponding to these values of journal bearing coefficients, values of K_{minor} were calculated for the journal bearings from Eq. (22) neglecting thrust bearing effects.

The critical speed map for rotor #1 is given in Figure 7. This figure shows the first two critical speed curves as a function of support stiffness. Also shown is a curve of the minor stiffness for the bearings calculated in the manner described above.

Whirl threshold speed is obtained from Figure 7 in the following way. First, if we draw an appropriate vertical line on Fig. 7 it will intersect both the first critical speed curve and the curve of K_{minor} vs. speed. Let us denote the values of speed at these intersections as ω_c and ω_T respectively. Now, corresponding to

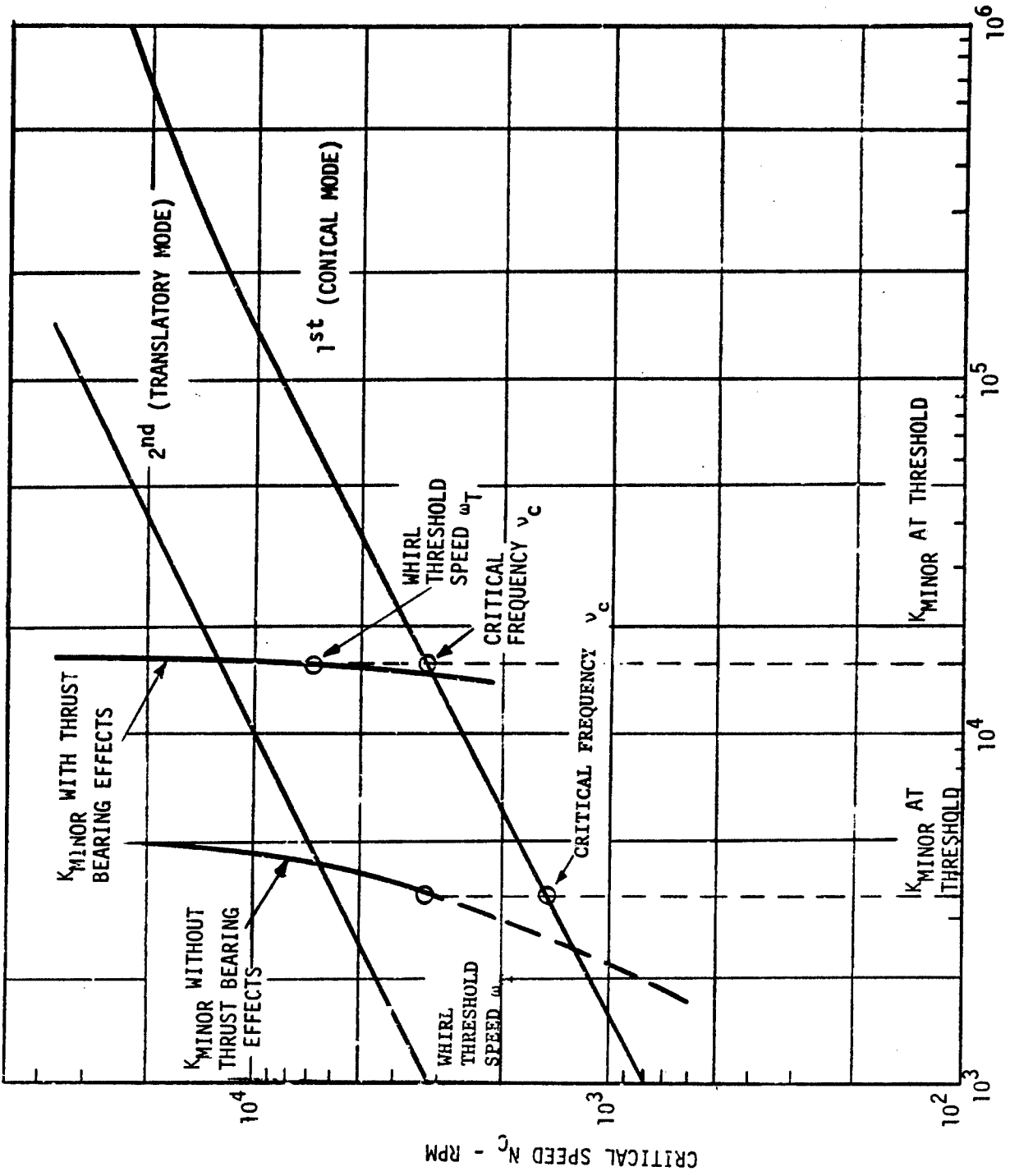


Fig. 7 Critical Speed Map of Rotor 1

these values of ν_c , the natural frequency of oscillation and ω_T , the rotor speed at which K_{minor} is calculated, there will be some value of whirl frequency ratio $\gamma = \nu/\omega$ calculable from Eq. (14). If this calculated value of γ is exactly equal to ν_c/ω_T , then we have determined the whirl threshold condition and ω_T will be our whirl threshold speed while ν_c/ω_T will be our whirl frequency ratio. If, say, ν_c/ω_T should prove to be less than our calculated value of γ , then we must try drawing another vertical line slightly further to the right and redetermine ν_c/ω_T . If ν_c/ω_T is less than the value of γ calculated from Eq. (14) then our new vertical line should be drawn slightly further to the left. Usually $\gamma \approx 0.5$ so we would first try drawing a vertical line such that $\nu_c/\omega_T = 0.5$.

In the example shown, neglecting thrust bearing effects, the whirl threshold speed is found to be $\omega_T = 3300$ rpm while the critical whirl frequency ratio is $\gamma = \nu_c/\omega_T = 0.457$.

It should be noted that in using this critical speed map approach, the curve of K_{minor} was calculated for the condition $\nu/\omega = 0.5$ rather than for the condition $\nu/\omega = 0.457$. For greater accuracy, one could recalculate K_{minor} at the predicted critical whirl ratio of 0.457 and redetermine the whirl threshold. Usually, however, this would result in only a very small change in the value of threshold speed and is not necessary.

Next let us consider how we would determine the threshold speed of rotor No. 1 in a more precise manner using the computer program PN400. In using the program, we can take advantage of the fact that we have already determined the threshold speed in an approximate manner by the critical speed map approach as described above. Therefore, with the computer program, we look for the roots of the real and imaginary parts of Eq. (10) in the vicinity of $\omega = 3300$ rpm and $\gamma = 0.457$.

The results obtained from the computer program are shown in Fig. 8. The straighter line represents the locus of roots of the imaginary part of Eq. (10), i.e., represents roots of Eq. (12), while the more curved line represents the locus of roots of the real part of Eq. (10), i.e., represents roots of Eq. (11). The intersection of these curves represents the condition at the threshold of whirl instability. As can be

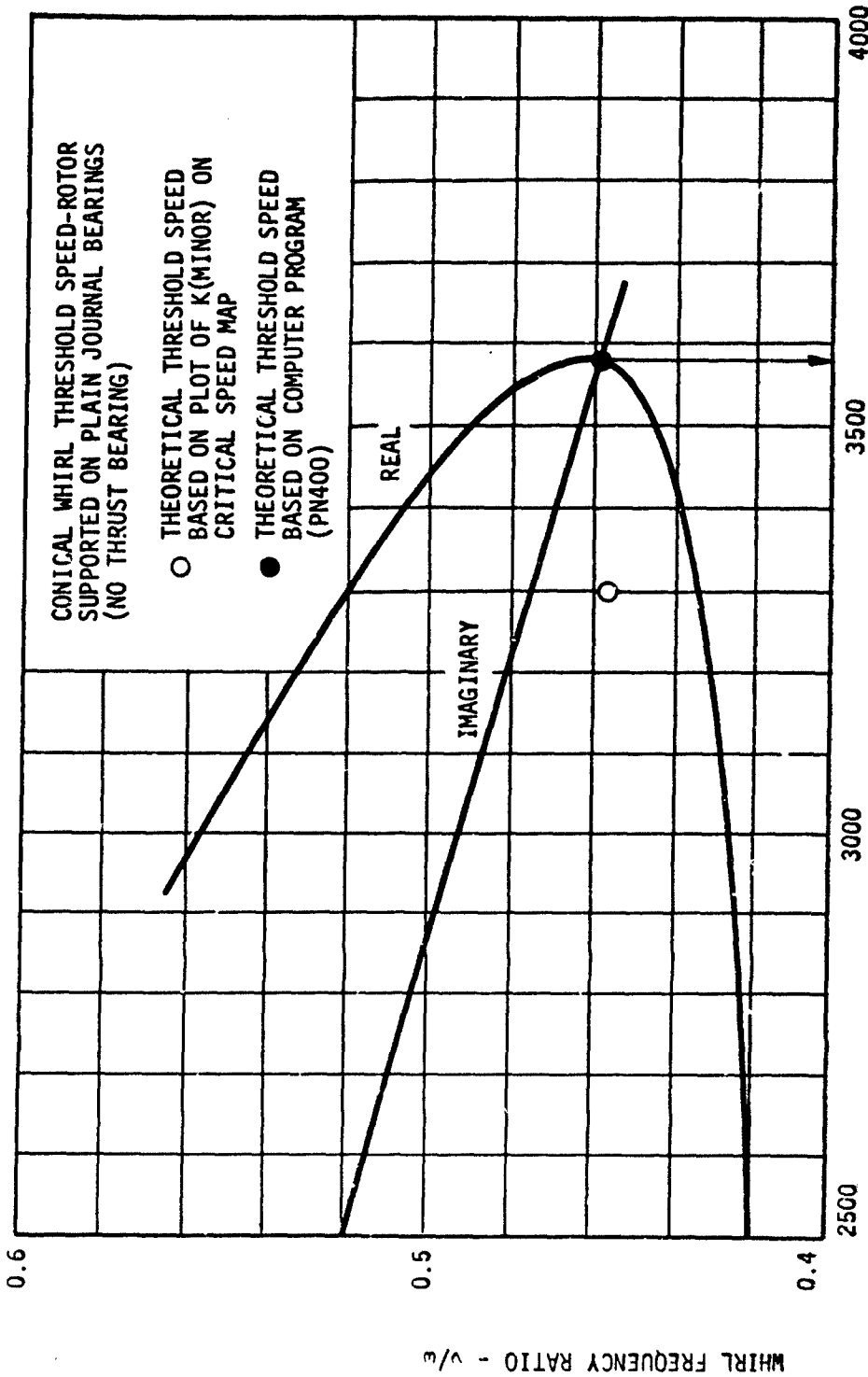


Fig. 8 Loci for Roots of Real and Imaginary Parts of Stability Determinant

seen, this occurs at a running speed of approximately 3570 rpm and at a frequency ratio of $\gamma = 0.460$.

For comparison, the whirl threshold solution obtained by the approximate critical speed map approach is also shown in Fig. 8. Agreement with the more precise computer solution is quite reasonable.

We can now proceed to investigate what change in the calculated value of whirl threshold speed for our example rotor No. 1 will result if we consider the thrust bearing angular stiffness and damping in our calculations. The thrust bearings for this rotor are hydrostatic with dimensions listed on page 25. In the case of hydrostatic thrust bearings, stiffness is the only bearing characteristic one usually needs consider in determining the influence of the thrust bearing on conical mode of whirl instability. This is so for the following reasons:

- (1) Damping, being the result of hydrodynamic forces rather than hydrostatic forces, is a very much weaker force in externally pressurized bearings than is the stiffness.
- (2) The "effective" angular damping in hydrostatic thrust bearings tends to zero at $\gamma \approx 0.5$ much the same as does the effective radial damping in plain cylindrical journal bearings. Hence, for whirl frequency ratios near 0.5, hydrostatic thrust bearing damping will be quite ineffective in increasing the threshold speed for conical whirl instability.

To determine the effects of the hydrostatic thrust bearing stiffness on our calculated value of whirl threshold speed, we will first do a rough calculation using the critical speed map approach and then do a refined calculation using computer program PN400. Data for the angular stiffness of hydrostatic thrust bearings is given in Figs. 13 through 16 in the next section as a function of the dimensionless feeding parameter A_s . As discussed in the next section, this data is for static or steady state displacement of the bearing. However, in most cases this is applicable to dynamic displacement of the bearing if the frequency ν of dynamic oscillation is low enough. To determine if steady state data is applicable, we

calculate the dimensionless squeeze number σ

$$\begin{aligned}\sigma &= \frac{12\nu v}{P_s} \frac{R_o R_1}{C^2} \\ &= \frac{12(2.7 \times 10^{-9}) v (.333)}{14.7(.0011)^2} \\ &= .605 \times 10^{-3} v\end{aligned}$$

At

$$\begin{aligned}N_t &= 3570 \text{ rpm} \\ \omega &= 373 \text{ rad/sec} \\ v &= (v/\omega)\omega \\ &= 187 \text{ rad/sec}\end{aligned}$$

Therefore

$$\sigma = .114$$

From Fig. 18, we see that squeeze number of $\sigma = 0.114$ is sufficiently low such that steady state values for bearing stiffness apply (see discussion of Figs. 17 and 18 in the next section).

To determine the angular stiffness G from Fig. 16, we must determine the dimensionless feeding parameter Λ_s . Our approach is to set Λ_s at the value yielding maximum stiffness i.e., $\Lambda_s \approx 1.0$. (This optimum value for Λ_s can be achieved for our bearing by the proper choice of na^2 in Λ_s .) The maximum value of dimensionless angular stiffness \bar{G} is

$$\frac{1 + \delta^2}{1 + 2/3 \delta^2} \bar{G} \approx .12$$

Now, our bearing is inherently compensated, so $\delta = a^2/cd$ is sufficiently large ($d = 2a$ and $c \ll a$) that the factor

$$\frac{(1 + \delta^2)}{(1 + 2/3 \delta^2)} \quad (\text{See References 7 and 8})$$

as $\delta \rightarrow \infty$ becomes approximately

$$\frac{\frac{1}{\delta^2} + 1}{\frac{1}{\delta^2} + \frac{2}{3}} = \frac{3}{2}$$

Solving for G from the expression given on Fig. 16 we have

$$G = \frac{\left[\left(\frac{1 + \delta^2}{1 + \frac{2}{3} \delta^2} \right) \bar{G} \right] \pi (R_o^2 - R_i^2) R_o^2 (P_s - P_a)}{\left(\frac{1 + \delta^2}{1 + 2/3 \delta^2} \right) C}$$

$$= \frac{12 \pi [(1)^2 - (.33)^2] (1)^2 (73.5 - 14.7)}{(3/2)(.00110)}$$

$$= 1.15 \times 10^4 \text{ in lb/radian}$$

As described earlier, this angular stiffness may be converted to an effective increase in journal bearing stiffness ΔK_e which can be added to the existing journal bearing stiffness for purposes of determining whirl threshold speed

$$\begin{aligned} \Delta K_e &= \frac{G}{L^2} \\ &= \frac{1.15 \times 10^4}{(1)^2} \\ &= 1.15 \times 10^4 \text{ lb/in.} \end{aligned}$$

For a hydrostatic thrust bearing, the cross-coupling terms are zero and the stiffness in the two principal planes are identical. Since K_{minor} is increased directly by increases in K_{xx} and K_{yy} , the equivalent increase in stiffness ΔK_e may be added directly to the K_{minor} obtained previously and the resultant curve for K_{minor} is plotted in Fig. 7. Using our graphical approach for determining whirl threshold speed, i.e., v_c/ω_T must equal γ calculated from Eq. (14), we find that the threshold speed with thrust bearings turns out to be at approximately 6900 rpm. Bearing stiffness and damping coefficients were therefore obtained for the hydrodynamic journal bearing at this value with $\bar{W} = 0.11$ using the $v/\omega = 0.50$ data. The journal bearing coefficients were then submitted along with the actual angular thrust bearing coefficients into the computer program. The results are shown plotted in Fig. 9 which yields a threshold speed of 7170 rpm at $v/\omega = 0.477$.

Rotor model No. 1 is an idealized model which serves as an example calculation of how thrust bearing stiffness may significantly improve the stability of the rotor to fractional frequency conical whirl instability, and how this improvement may be calculated. In rotor model No. 2 we have an example of an actual prospective design for a high temperature turbocompressor which was rejected on the basis of its poor stability characteristics. A simplified drawing of the rotor is shown in Fig. 6 and a brief description of the rotor was given earlier in this section. Due to the overhung nature of the design, the lowest mode of fractional frequency whirl instability was conical in nature. However, since the analytical tools were not available at the time this design was proposed, no account was taken of the effect of the thrust bearing in possibly enhancing the rotor stability. We shall examine the stabilizing influence of this thrust bearing in what follows below.

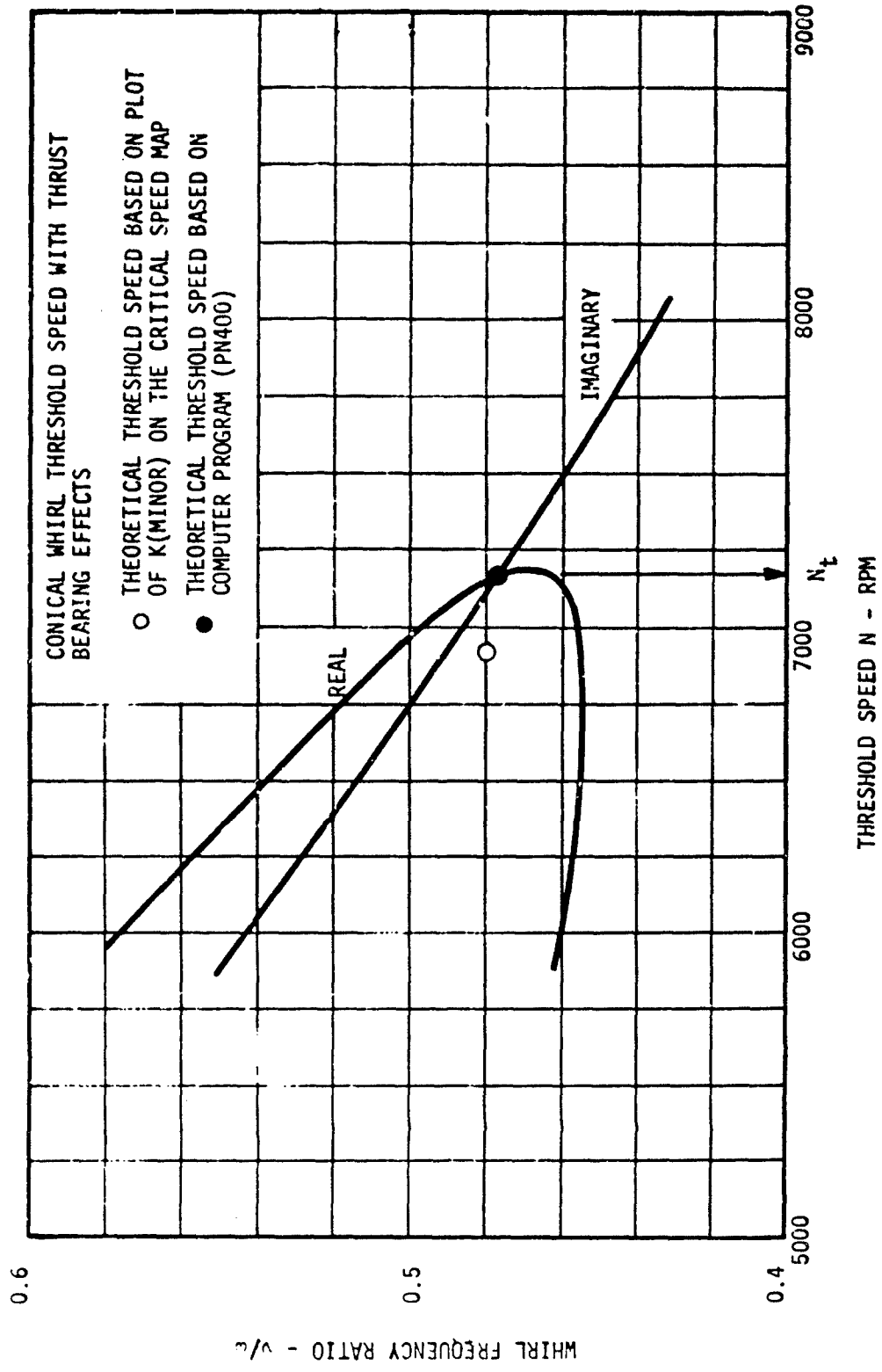


Fig. 9 Loci of Roots for Real and Imaginary Parts of Stability Determinant

The data for rotor No. 2 are as follows:

Rotor Model #2

Journal Bearing Design (Hybrid)

D = 3.00 in.	R = 2.472 x 10 ⁵ in. ² /sec ² °R
L = 3.25 in.	n = 32 holes
C = .0026 in.	a = .012 in. (orifice radius)
P _a = 18 psia	Orifice compensation
P _s = 72 psia	Single Plane Admission
W = 6.95 lb. (No. 1 bearing), 11.80 lb. (No. 2 bearing)	
μ = 3.40 x 10 ⁻⁹ lb. sec./in. ²	
T = 760°R	

Thrust Bearing Design (Hydrostatic)

R _o = 2.53 in.	M = 3.35 x 10 ⁻⁹ lb.sec./in. ²
R _i = 1.55 in.	C = .0015 in.
P _a = 18 psia	n = 40 holes
P _s = 30.6 psia	a = .030 in. = d/2 (inherently compensated)
T _s = 1150°R	δ = a ² /cd = 10

Table II gives the hybrid gas-lubricated journal bearing data for an L/D = 1.08 with v/ω = 0.50 at P_s/P_a = 4.0. The hydrostatic effect parameter Λ_s for the journal bearing design with orifice compensation (δ = 0) and single plane admission is given by:

$$\Lambda_s = \frac{6\mu n a^2 \sqrt{RT}}{P_s C^3 \sqrt{1 + \delta^2}}$$

$$= \frac{(6)(3.4 \times 10^{-9})(32)(.012)^2 \sqrt{2.472 \times 10^5 \times 760}}{(72)(.0026)^3}$$

$$= 1.025$$

The data in Table II are applicable for $\Lambda_s = 1.0$ with the only variables being the hydrodynamic effects Λ and load capacity \bar{W} . Again double interpolation is required to obtain the necessary stiffness and damping coefficients at a constant \bar{W} value. The \bar{W} values for rotor No. 2 are

Journal Bearing Data

$$\begin{aligned}\bar{W}_1 &= \frac{W_1}{P_a LD} \\ &= \frac{6.95}{18(3.25)(3)} \\ &= .0396 \quad (\text{bearing 1})\end{aligned}$$

$$\begin{aligned}\bar{W}_2 &= \frac{W_2}{P_a LD} \\ &= \frac{11.8}{18(3.25)(3)} \\ &= .0672 \quad (\text{bearing 2})\end{aligned}$$

The relationship between bearing number Λ and rotational speed N is:

$$\begin{aligned}\Lambda &= \frac{12\pi N}{P_a} \left(\frac{R}{C} \right)^2 \\ &= \frac{12\pi(3.4 \times 10^{-9})N}{18} \left(\frac{1.500}{.0026} \right)^2 \\ &= 2.38 \times 10^{-3} N \quad (\text{where } N = \text{rps}) \\ &= 3.96 \times 10^{-5} N' \quad (\text{where } N' = \text{rpm})\end{aligned}$$

The bearing data shown in Table III are obtained from Table II, by interpolation, for $\bar{W}_1 = .0396$ and $\bar{W}_2 = .0672$. The values of K_{minor} given in Table III are calculated from Eq. (18) or Eq. (22). The values of $\gamma = v/\omega$, the frequency ratio at which effective damping goes to zero, are calculated from Eq. (14).

The critical speed curves for rotor No. 2 are plotted in Figure 10. Also plotted is the curve of K_{minor} vs. speed. In this case K_{minor} varies hardly at all with speed, which makes calculation of the whirl threshold speed ω_T , very easy. Noting that for instability v_c/ω_T must equal γ (which in this case is very nearly exactly 0.5) and noting that v_c can now be given by the intersection of the curve of K_{minor} with the lowest critical speed curve, we have

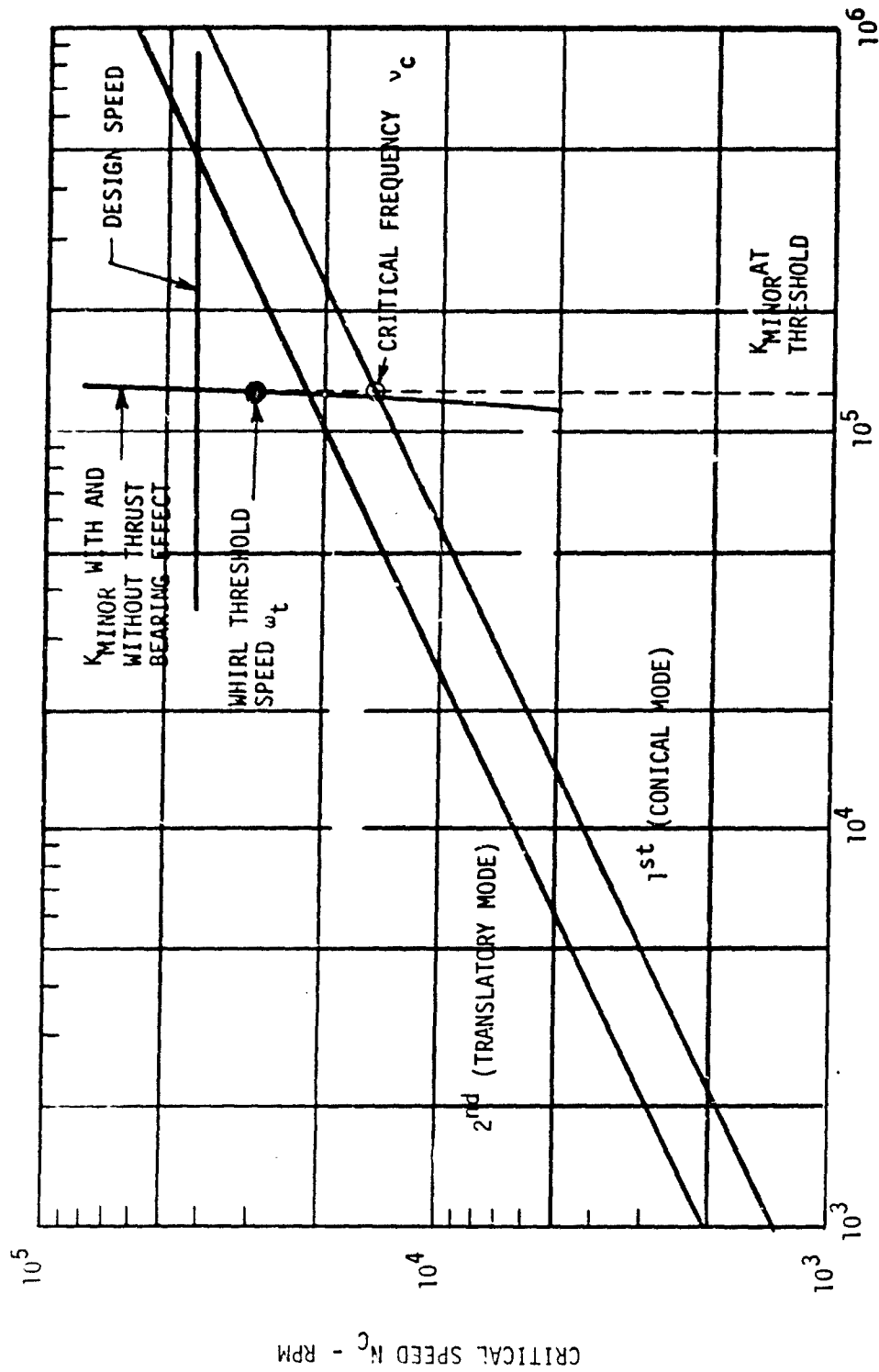
$$v_c = 14,750 \text{ rpm (from Figure 10)}$$

$$\omega_T = v_c/0.5 = 29,500 \text{ rpm}$$

To obtain a more exact calculation for ω_T , we use computer program PN400 with bearing input data obtained from Table III. The results obtained are shown in Fig. 11. The approximate solution obtained above from the critical speed map approach is shown as a circle in Figure 11. The solution curves for the real and imaginary parts of the stability determinant being equal to zero (the solution curves for Eq. (11) and (12)) are very nearly parallel for this example, making exact determination of the whirl threshold speed quite difficult. As can be seen, the whirl threshold speed lies somewhere in the range of 29,000 to 29,375 rpm and the whirl frequency ratio is between 0.499 and 0.504.

Next we compute the effect of the thrust bearing on this whirl threshold speed. Using the thrust bearing design data, the squeeze number σ evaluated at the previous calculated value of v_c , the oscillation frequency at whirl threshold is

$$\begin{aligned} \sigma &= \frac{12\mu v}{P_a} \left(\frac{R_i R_o}{c^2} \right) \\ &= \frac{12(3.35 \times 10^{-9})(1540)(2.53)(1.55)}{18 (.0015)^2} \\ &= 6.0 \end{aligned}$$



BEARING STIFFNESS K - lb/in

Fig. 10 Critical Speed Map of Rotor 2

TABLE III

HYBRID GAS BEARING DATA

$L/D = 1.08 \quad P/P_g = 4.0$

\bar{W}	A	N	γ/ω	\bar{K}_{minor}	K_{minor} (lb/in)	K_{xx} (lb/in)	K_{xy} (lb/in)	K_{yx} (lb/in)	K_{yy} (lb/in)	ω_B_{xx} (lb/in)	ω_B_{xy} (lb/in)	ω_B_{yx} (lb/in)	ω_B_{yy} (lb/in)
.0396	.50	12400	.500	1.804	1.22×10^5	1.22×10^5	5.06×10^3	5.06×10^3	1.22×10^4	1.02×10^4	8.70×10^2	8.70×10^2	1.02×10^4
	1.00	24800	.499	1.808	1.22×10^5	1.24×10^5	9.92×10^3	9.99×10^3	1.24×10^4	2.00×10^4	3.57×10^3	3.57×10^3	2.00×10^4
	1.75	43400	.499	1.806	1.22×10^5	1.28×10^5	1.62×10^4	1.62×10^4	1.27×10^4	3.23×10^4	1.03×10^4	1.03×10^4	3.24×10^4
	3.00	74500	.492	1.812	1.22×10^5	1.35×10^5	2.35×10^4	2.35×10^4	1.35×10^4	4.72×10^4	2.60×10^4	2.61×10^4	4.72×10^4
	5.00	124000	.500	1.809	1.22×10^5	1.48×10^5	2.78×10^4	2.79×10^4	1.48×10^4	5.76×10^4	5.12×10^4	5.11×10^4	5.58×10^4
.0672	.50	12400	.500	1.811	1.22×10^5	1.23×10^5	5.06×10^3	5.06×10^3	1.23×10^4	1.02×10^4	8.70×10^2	8.70×10^2	1.02×10^4
	1.00	24800	.499	1.812	1.22×10^5	1.24×10^5	9.92×10^3	9.99×10^3	1.24×10^4	1.99×10^4	3.57×10^3	3.57×10^3	2.00×10^4
	1.75	43400	.499	1.804	1.22×10^5	1.27×10^5	1.61×10^4	1.61×10^4	1.27×10^4	3.24×10^4	1.03×10^4	1.04×10^4	3.24×10^4
	3.00	74500	.512	1.809	1.23×10^5	1.35×10^5	2.36×10^4	2.31×10^4	1.35×10^4	4.71×10^4	2.60×10^4	2.60×10^4	4.72×10^4
	5.00	124000	.499	1.809	1.22×10^5	1.48×10^5	2.79×10^4	2.79×10^4	1.48×10^4	5.31×10^4	5.11×10^4	5.11×10^4	5.58×10^4

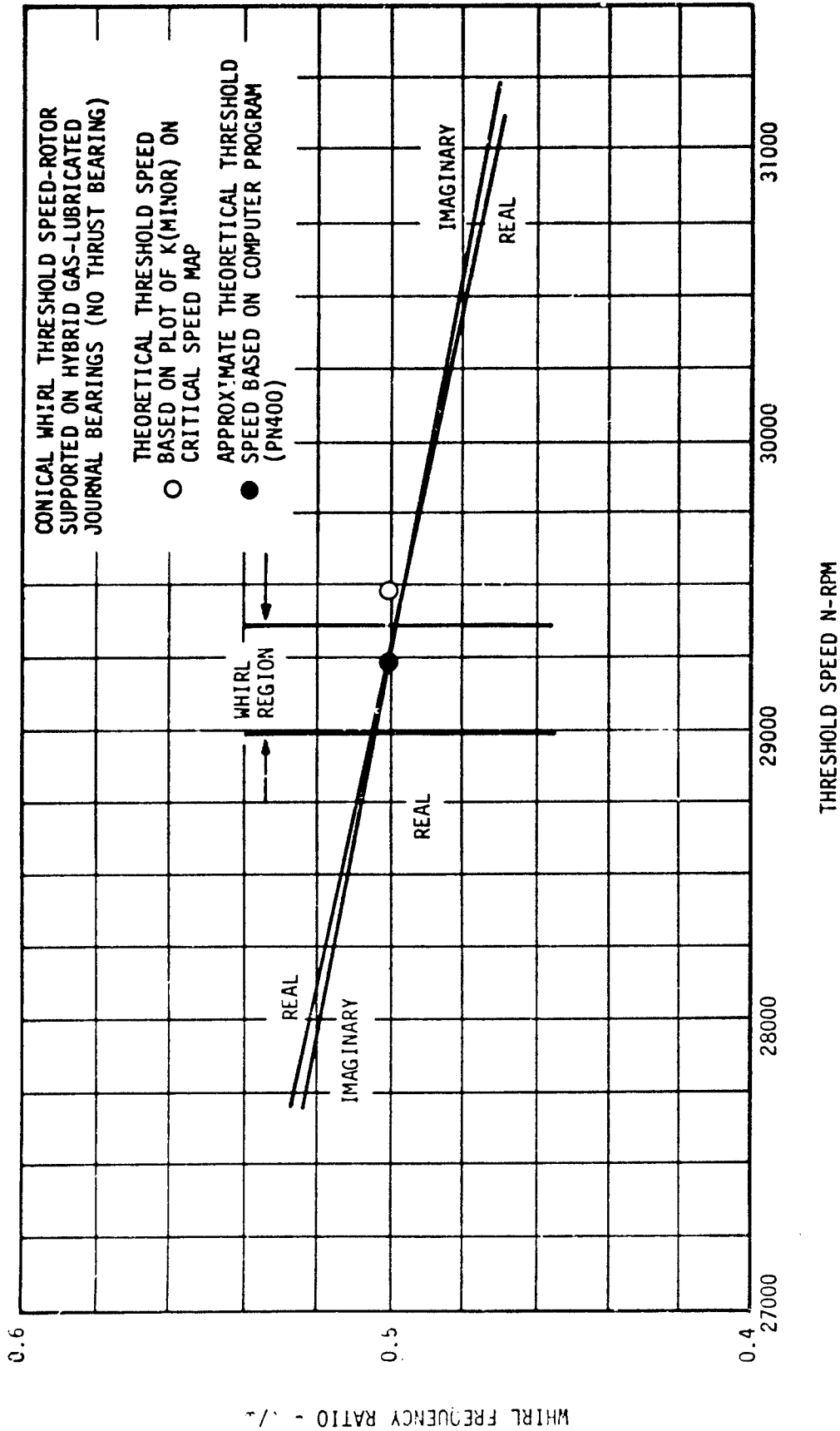


Fig. 11 Loci of Roots for Real and Imaginary Parts of Stability Determinant

The restrictor coefficient Λ_s equals:

$$\begin{aligned} \Lambda_s &= \frac{6\mu n s^2 \sqrt{RT}}{P_s C^3 \sqrt{1 + \delta^2}} \\ &= \frac{(6)(3.35 \times 10^{-9})(40)(.03)^2 \sqrt{2.472 \times 10^5 \times 1150}}{(30.6)(.0015)^3 \sqrt{1 + 10^2}} \\ &= 11.80 \end{aligned}$$

This value of Λ_s is significantly higher than the optimum value for maximum bearing stiffness (see Figure 15). This is because the operating condition being analyzed is the one at which stability of the rotor is poorest and is not the operating condition for which the bearing was designed. The curve of dynamic stiffness shown in Fig. 17 pertain to a value of $\Lambda_s = 2.5$ which is optimum for a thrust bearing of radius ratio of $R_o/R_i = 1.5$. From this curve we see that such a bearing, operating at a squeeze number of $\sigma = 6.0$ would be well within the range where steady state stiffness data apply; i.e., is operating at an oscillation frequency which is well below the frequency at which squeeze film effects become important. Physically, there is no reason to expect that this situation would be altered significantly when the bearing is operated at higher Λ_s (i.e., lower supply pressure). Therefore, we would readily expect that our example bearing at $\Lambda_s = 11.8$ and $\sigma = 6.0$, would be in the "steady state" region where Fig. 15 could be used to calculate bearing stiffness. From Fig. 14, at $P_s/P_a = 1.70$, we determine that

$$\frac{1 + \delta^2 \bar{G}}{1 + 2/3 \delta^2} = 0.07$$

$$\bar{G} = (.07) \frac{1 + 2/3 \delta^2}{1 + \delta^2} = (.07) \frac{1 + 2/3 (10)^2}{1 + (10)^2}$$

$$= .0469$$

$$\begin{aligned}
G &= \frac{\pi(R_o^2 - R_i^2) R_o^2 (P_s - P_a) \bar{G}}{c} \\
&= \frac{\pi [(2.53)^2 - (1.55)^2] (2.53)^2 (30.6 - 18)(.0469)}{.0015} \\
&= 3.02 \times 10^4 \text{ in.lb/rad.}
\end{aligned}$$

Since we have only one thrust bearing, we must appropriately divide its effect among the two journal bearings to use the effective stiffness - critical speed map approach for approximately calculating the effect of the thrust bearing on whirl threshold speed. The distance of journal bearings 1 and 2 from the c.g. of the rotor are $L_1 = 4.72''$ and $L_2 = 2.78''$ respectively. By analogy with Eq. (29), which gives the relationships for adding an effective stiffness of one thrust bearing to one journal bearing, we can infer that a correct approach for adding an effective stiffness of one thrust bearing of angular stiffness G to two journal bearings of spans L_1 and L_2 would be by the relationship

$$K_e = \frac{G}{L_1^2 + L_2^2}$$

Therefore, the effective radial stiffness to be added to each journal bearing would be

$$\begin{aligned}
K_e &= \frac{G}{L_1^2 + L_2^2} \\
&= \frac{3.02 \times 10^4}{30} \\
&= 1010 \text{ lb/in}
\end{aligned}$$

This value is seen to be negligible compared with the values of stiffness associated with the journal bearings themselves. Hence, in this case, the thrust bearing would have negligible effect on conical motions of the shaft.

The above conclusion reached for rotor No. 2 probably pertains to most rotor designs. In general, such rotors will be designed so that the span between journal bearings is sufficiently great that these bearings will exert a much greater restraining force on conical motions of the shaft than will the thrust bearings. However, this need not always be true. It is easy to conceive of systems where the thrust loads dominate and where journal bearings are needed only to locate the shaft. In such systems a designer could take advantage of the now available technology for including thrust bearing effects in whirl threshold speed calculations, and design the rotor such that the thrust bearing could assume the responsibility of restraining conical motions of the rotor.

SECTION IV

ANGULAR STIFFNESS COEFFICIENTS FOR HYDROSTATIC THRUST BEARINGS

The hydrostatic bearing data presented in this section are based on an analysis by Lund described in Reference [5]. Basically, the analysis involves the assumption that discrete feeding holes arranged in an annular thrust bearing (see Fig. 12) can be represented approximately by a continuous "line source" of feeding as if the bearing were fed by a continuous circular slot rather than by discrete holes. This approximation tends to be absolutely correct in the limit as the number of feeding holes approaches an infinite number, but tends to somewhat overestimate bearing load and stiffness for bearings having a finite number of holes. A line source correction factor to account for this overestimation has been worked out by comparing a detailed discrete feeding analysis with the simpler line source analysis. The correction factor to be applied depends on the product $n\xi$ and $d/\xi D$ where n is the number of feeding holes, $\xi = 1/2 \log_e (R_o/R_i)$, d is the diameter of the feeding holes, $D = 2 \sqrt{R_o R_i}$, R_o and R_i are the outer and inner radii of the thrust bearings having a practical number of holes, the correction factor to be applied is $2/3$, i.e., the line source analysis overestimates the stiffness by 50%. This correction factor has been built into the design curves presented in this section. Figure 19 shows a curve of $n\xi$ vs. $d/\xi D$ giving the recommended size and number of feedings for which this correction applies. If more feeding holes are used, stiffness will be higher than that predicted by the design charts in this section and conversely.

The stiffness of compressible hydrostatic bearings is dependent upon the frequency of excitation ν of the bearing if this frequency is high enough. This is because, at large values of ν , the gas in the bearing film tends to be dropped and compressed rather than squeezed out of the film, and this contributes to a higher level of bearing stiffness. This effect is illustrated in figures 17 and 18 where dimensionless stiffness $\bar{G} = CG/[\pi(R_o^2 - R_i^2) R_o^2 (P_s - P_a)]$ is plotted vs. the dimensionless excitation frequency σ (known as squeeze number)

$$\tau = \frac{12.5\nu}{P_s} \left(\frac{R_i R_o}{C^2} \right)$$

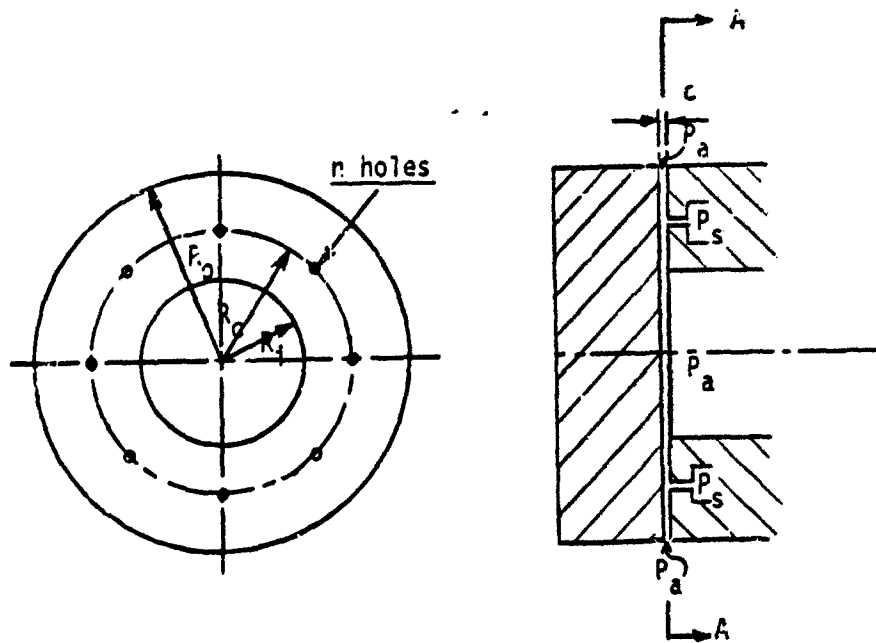


Fig. 12 Sketch of Hydrostatic Thrust Bearing

as can be seen, for small σ , the stiffness remains constant at its steady state value independent of excitation frequency. However, once ν becomes large enough, the bearing stiffness begins to increase with ν due to the above mentioned squeeze film effect.

In general, for rotors supported on hydrostatic bearings, the running speed will be in the range such that an excitation frequency $\nu \approx \omega/2$ will lead to squeeze numbers sufficiently low such that steady state bearing stiffness data will apply. This is generally so because if shaft speeds are high enough such that compressibility becomes significant in the squeeze film effect, then the shaft speed will tend to be high enough such that hydrodynamic bearings could be used for load support. Figures 17 and 18 will be used, therefore, primarily to define the limits below which steady state bearing data apply rather than being used as a source of dynamic stiffness data.

In Figures 13 through 16 are presented dimensionless angular stiffness \bar{G} vs. the feeding parameter Λ_s

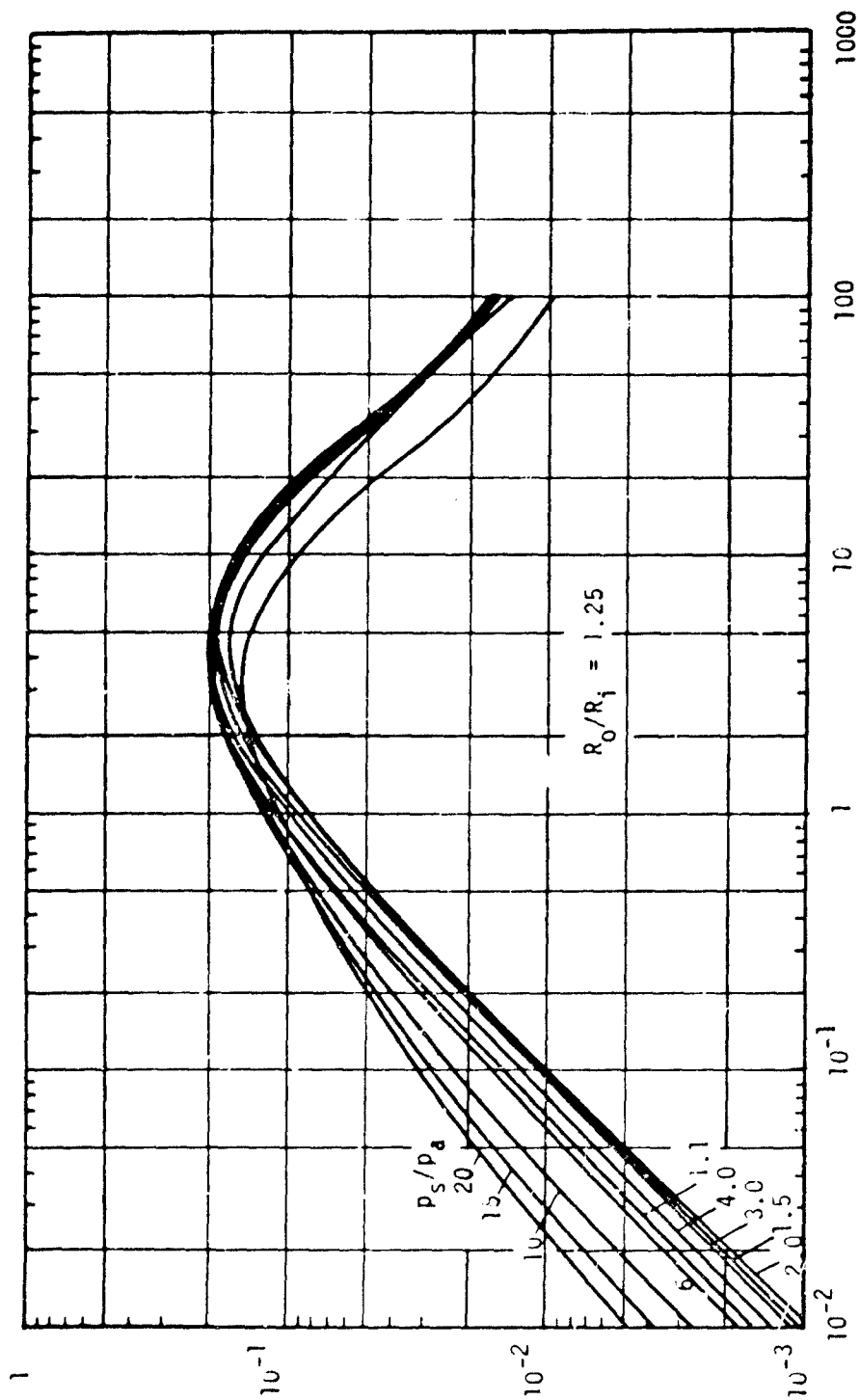
$$\Lambda_s = \frac{6.4 \pi a^2 \sqrt{RT}}{P_s C^3 \sqrt{1 + \delta^2}} \quad (31)$$

for radius ratios of $R_o/R_i = 1.25, 1.5, 2.0, \text{ and } 3.0$. The dimensionless stiffness \bar{G} is pre-multiplied by the factor $1 + \delta^2/(1 + 2/3 \delta^2)$ where $\delta = a^2 cd$, known as the inherent compensation factor, gives the ratio of orifice area πa^2 to inherent restriction area πcd (see Figure 12). Curves are provided for different values of pressure ratio P_s/P_a . Usually, the hydrostatic thrust bearings are designed for a value of Λ_s which provides near maximum stiffness; i.e., Λ_s is in the range 1.0 to 4.0, depending on radius ratio. Hence, the dynamic curves in Figs. 17 and 18 are presented for near optimum values of Λ_s .

Only stiffness data is provided for the hydrostatic bearings. This is for the following reasons:

- (1) Damping in hydrostatic bearings results, essentially, from hydrodynamic forces which are usually much weaker than the hydrostatic forces producing bearing stiffness.

- (2) More importantly, in hydrostatic thrust bearings, "effective" bearing damping tends to zero for wobbling or nutating modes of motion which occur at half the rotational speed of the thrust runner. In examining the stability of rotors, it is invariably the influence of precisely this kind of thrust bearing motion on rotor dynamics that we are attempting to calculate. Hence in such calculations, it is quite reasonable to presume that the effects of thrust bearing damping will be zero or near zero and only consider the effects of thrust bearing stiffness.

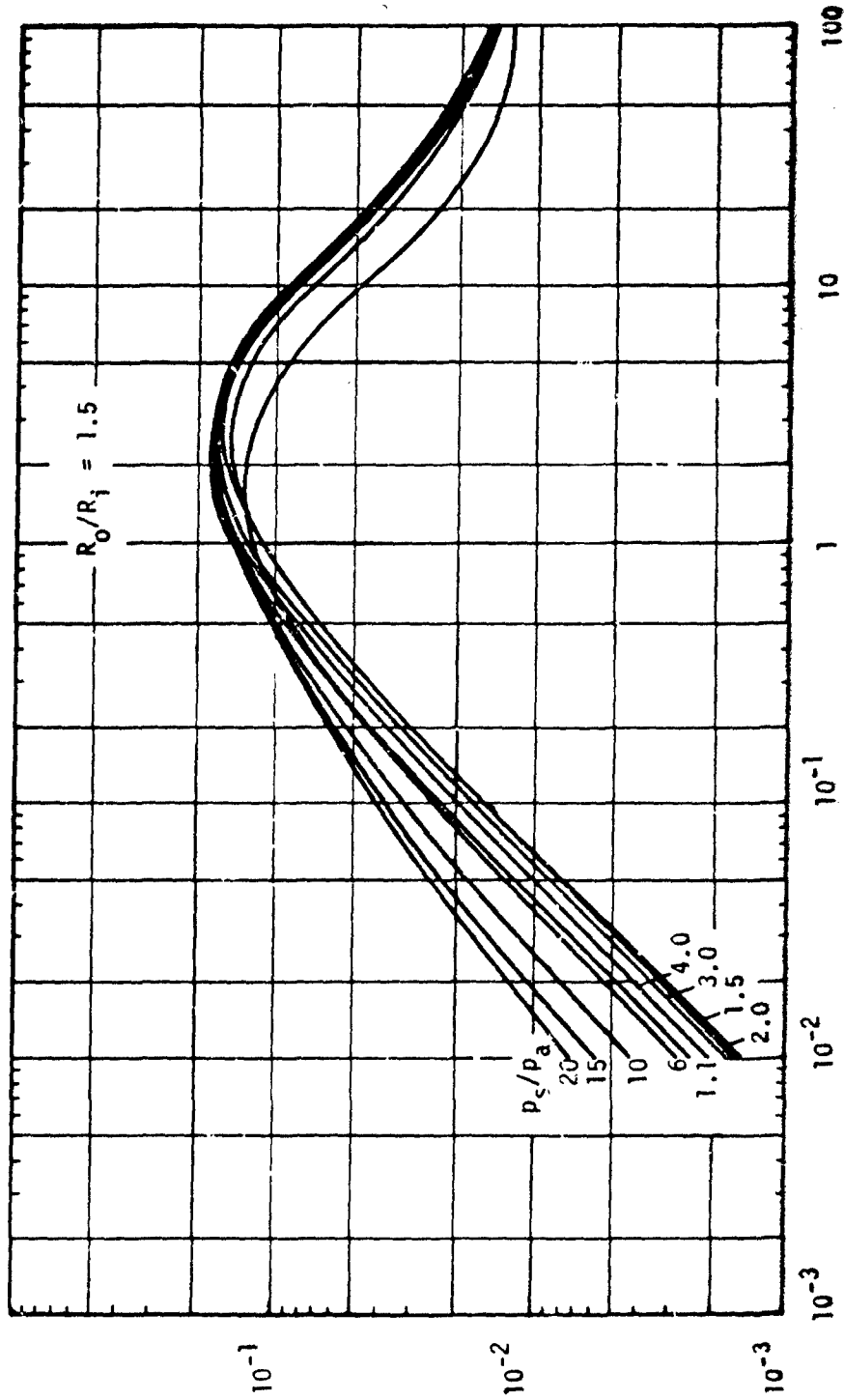


$$\Lambda_S = \frac{6\mu n a^2 \sqrt{RT}}{P_S C^3 \sqrt{1 + \delta^2}}$$

Fig. 13 Hydrostatic Thrust Bearing, $R_0/R_i = 1.25$
Dimensionless Angular Stiffness vs. Restrictor Coefficient

$$\frac{1 + \frac{\delta^2}{2}}{1 + \frac{\delta^2}{2/3}} = \frac{1 + \frac{\delta^2}{2}}{1 + \frac{\delta^2}{2/3}} \cdot \frac{1 + \frac{\delta^2}{2}}{1 + \frac{\delta^2}{2}} = \frac{(1 + \frac{\delta^2}{2})^2}{1 + \frac{\delta^2}{2/3}}$$

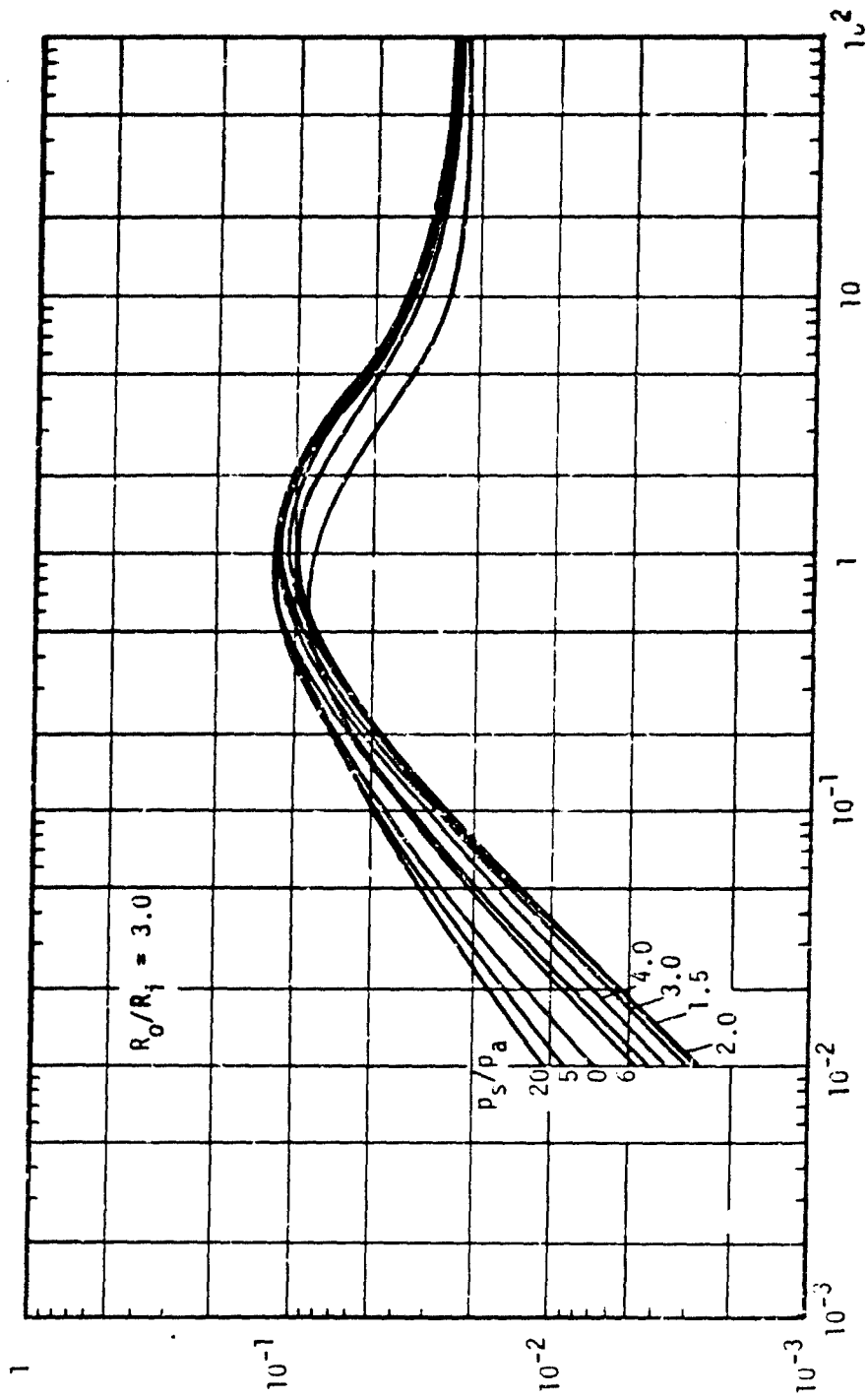
$$\frac{1 + \delta^2}{1 + 2/3 \delta^2} = \frac{1 + \delta^2}{1 + 2/3 \delta^2} \cdot \frac{\pi(R_0^2 - R_i^2)R_0^2(p_s - p_a)}{CG} = \frac{1 + 2/3 \delta^2}{1 + \delta^2} \pi(R_0^2 - R_i^2)R_0^2(p_s - p_a)$$



$$\lambda_s = \frac{6\mu n a^2 \sqrt{RT}}{P_s C^3 \sqrt{1 + \delta^2}}$$

Fig. 14 Hydrostatic Thrust Bearing, $R_0/R_i = 1.5$
Dimensionless Angular Stiffness vs. Restrictor Coefficient

$$\frac{1 + \frac{\delta^2}{2}}{1 + \frac{2/3 \delta^2}{2}} = \frac{1 + \frac{\delta^2}{2}}{1 + \frac{2/3 \delta^2}{2}} = \frac{1 + \frac{\delta^2}{2}}{1 + \frac{2/3 \delta^2}{2}} = \frac{1 + \frac{\delta^2}{2}}{1 + \frac{2/3 \delta^2}{2}}$$



$$\Lambda_S = \frac{6\mu n a^2 \sqrt{RT}}{P_S C^3 \sqrt{1 + \delta^2}}$$

Fig. 16 Hydrostatic Thrust Bearing, $R_0/R_i = 3$
Dimensionless Angular Stiffness vs. Restrictor Coefficient

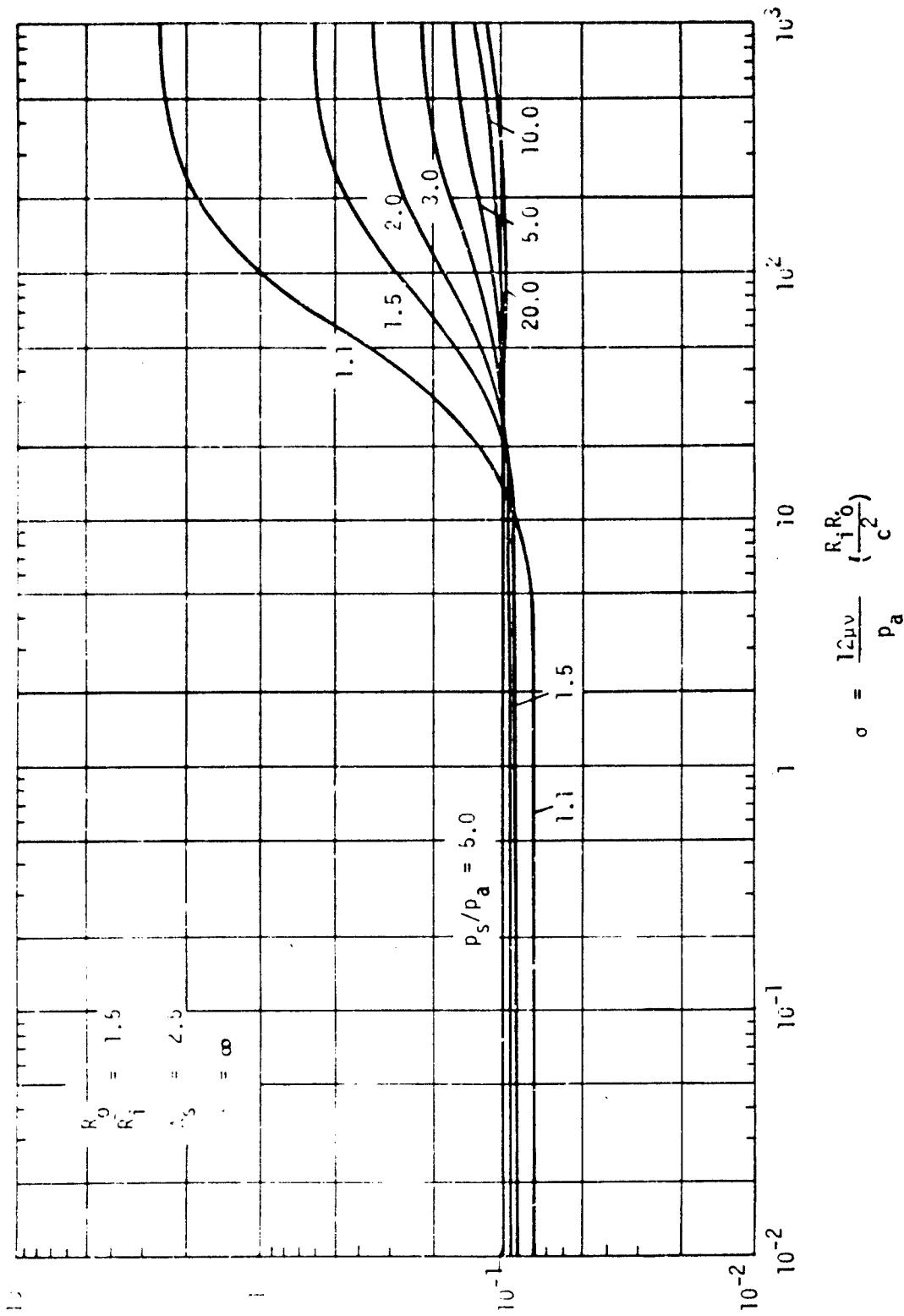


Fig. 17 Dynamic Angular Stiffness for the Hydrostatic Thrust Bearing
 $R_0/R_1 = 1.5$. Inherent Compensation

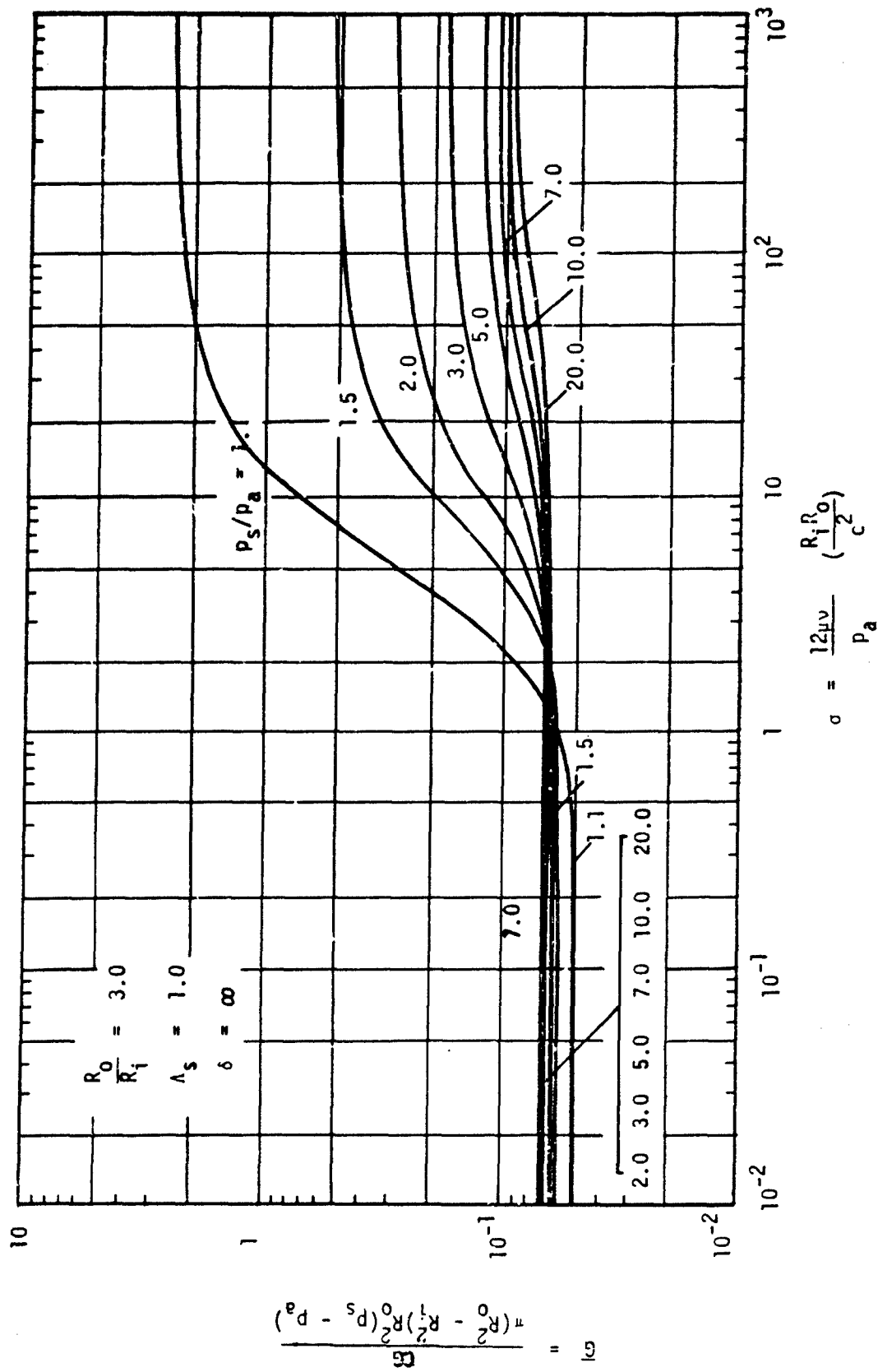


Fig. 18 Dynamic Angular Stiffness for the Hydrostatic Thrust Bearing
 $R_0/R_i = 3.0$ Inherent Compensation

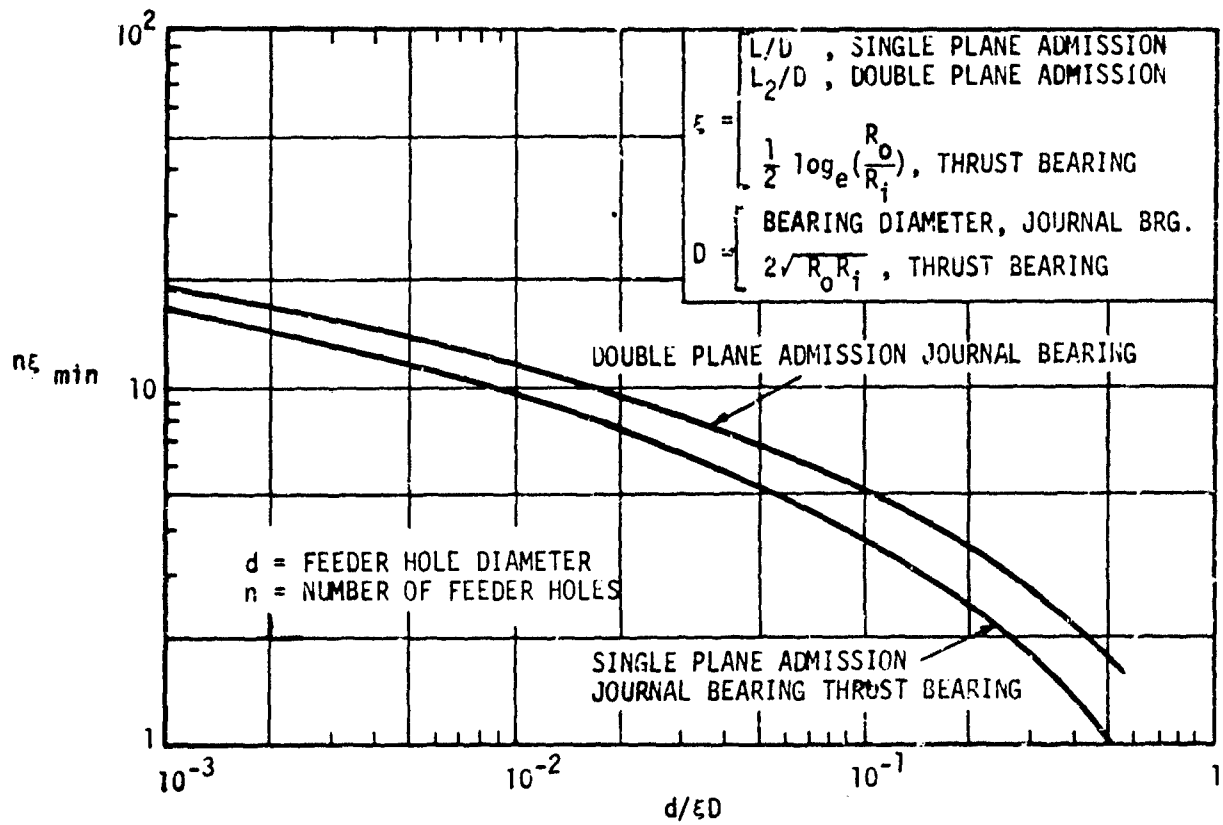


Fig. 19 Minimum Number of Feeder Holes

APPENDIX I
COMPUTER PROGRAM
THE THRESHOLD OF INSTABILITY OF A FLEXIBLE ROTOR IN FLUID FILM BEARINGS

This section describes the rotor stability computer program PN400: "The Threshold of Instability of a Flexible Rotor in Fluid Film Bearings". This program is quite similar to the computer program PN0017 given in Reference 1.

The new program described in this volume is a modification and extension of the previous version. The amount of plotting has been significantly reduced in that a quadratic interpolation¹ routine now automatically performs much of the plotting previously required to find the zero point solutions for both the real and imaginary parts of the complex determinant. This program also now accepts the angular thrust bearing properties and is also set up to handle both liquid-lubricated and gas-lubricated bearings. In addition a more refined rotor model is employed which describes the rotor in terms of stiffness and mass diameters, lengths, concentrated values of mass, and mass moments of inertia. The new rotor model is discussed in Reference 3.

Analysis

The rotor analysis is described in detail in Reference 3, Appendix VIII. Consider the rotor shown in Fig. 3 and assuming the two ends of the rotor to be free, the bending moment and the shear force at one rotor end are directly proportional to the unknown amplitude and slope at the opposite rotor end. The proportionality coefficients are the dynamic influence coefficients which are computed by the program, and the final equation is given in the following matrix form (see Eq. (H.61) in Appendix VIII of Reference 3 neglecting magnetic influence coefficient matrix).

¹ Second-order polynomial interpolation. See Reference 6.

$$\begin{Bmatrix} V'_{xm} \\ V'_{ym} \\ M'_{xm} \\ M'_{ym} \end{Bmatrix} = \begin{Bmatrix} a_{11} & a_{12} & a_{13} & a_{14} \\ a_{21} & a_{22} & a_{23} & a_{24} \\ a_{31} & a_{32} & a_{33} & a_{34} \\ a_{41} & a_{42} & a_{43} & a_{44} \end{Bmatrix} \begin{Bmatrix} x_1 \\ y_1 \\ \theta_1 \\ \phi_1 \end{Bmatrix} \quad (32)$$

Here, V'_{xm} and V'_{ym} are the shear force components at one rotor end (station m), M'_{xm} and M'_{ym} are the bending moment components at the same location, and x_1 , y_1 , θ_1 and ϕ_1 are the unknown amplitudes and slopes at station 1. The a's are the dynamic influence coefficients which depend on the whirl frequency ratio and the rotor speed. They include the effect of rotor inertia, rotor flexibility and the dynamic bearing coefficients. Since the ends of the rotor are free, $V'_{xm} = V'_{ym} = M'_{xm} = M'_{ym} = 0$. Thus, x_1 , y_1 , θ_1 and ϕ_1 are only different from zero when the determinant of the matrix of influence coefficients is zero which, then, determines the threshold of instability:

$$\Delta = \Delta_c + i\Delta_s = \begin{vmatrix} a_{11} & a_{12} & a_{13} & a_{14} \\ a_{21} & a_{22} & a_{23} & a_{24} \\ a_{31} & a_{32} & a_{33} & a_{34} \\ a_{41} & a_{42} & a_{43} & a_{44} \end{vmatrix} = 0 \quad (33)$$

For each given angular speed, ω , of the rotor, the program calculates Δ_c and Δ_s for specified values of the whirl frequency ratio $\gamma = \nu/\omega$ and determines the zero points of Δ_c and Δ_s within the given range. The results can be plotted directly to find the threshold of instability.

COMPUTER INPUT

Card 1 (72H)

Any descriptive text may be given to identify the calculation.

Card 2 (14I5)

This is the "control card" whose values control the rest of the input. The control card has 10 items:

1. NS, the number of rotor stations, see "Rotor Data" ($1 \leq NS \leq 100$)

2. NB, the number of bearings ($1 \leq NB \leq 10$)

3. NPST. The program provides for including the response characteristics of the bearing pedestals. When it is desired to include this effect, set NPST = 1 and give the required input data as explained later. When NPST = 0, the pedestals are assumed to be rigid and no pedestal data are required in the input.

4. NANG. The dynamic forces of the fluid film in the journal bearings resist both radial motion and angular motion. In most cases, only the radial forces are significant in which case NANG is set equal to zero. However, long journal bearings and especially thrust bearings may exert considerable constraint on the angular motion of the rotor. When it is desired to include this effect, set NANG = 1 and give the required input data as explained later.

5. NFR is the number of whirl frequency ratios specified in the input list below, see explanation later ($3 \leq NFR \leq 50$).

6. INC. If the bearing lubricant is compressible (gas bearings), set INC = 1 in which case the dynamic bearing coefficients must be specified for each whirl frequency ratio in the input. If INC = 0, the lubricant is incompressible and the dynamic bearing coefficients are independent of whirl frequency.

7. NIT. As discussed previously, the program searches for the zero points of the instability determinant. To do this, the instability determinant is computed as a function of the whirl frequency ratio. The input gives NFR values of the whirl frequency ratio in sequence, and the determinant is calculated for each of these values. In addition, each interval is subdivided into NIT increments and the determinant is also computed at these intermediate frequency ratio values. Whenever the program detects a change in sign of the determinant between two consecutive calculations, it uses quadratic interpolation to find the accurate zero point.

By subdividing the intervals in the given frequency ratio list, the list can be shortened without loss of accuracy. Furthermore, when the bearing lubricant is a gas it is necessary to provide the dynamic coefficients for each specified frequency ratio. Thus, to minimize the input data it is desirable to keep this number low. Then the program automatically calculates the coefficients for the intermediate points by quadratic interpolation.

NIT should be equal to or greater than 1. When NIT = 1, no subdivision takes place.

8. METR. This item should always be zero. It is included for diagnostic purposes which, however, is of no value to the general user of the program.

9. NCAL, specifies the number of rotor speed ranges. For each speed range it is necessary to give input data for the dynamic bearing coefficients. There is no limit for NCAL.

10. INP. If INP = 0, the present set of input data is followed by a new set, starting from Card 1. If INP = 1, this is the last set of input.

Card 3 (1F6E12.5)

1. YM is Young's modulus E for the shaft material in lbs/inch^2 . If E actually changes along the rotor it should be noted that the program only uses E in the product EI where I is the cross-sectional moment of inertia of the shaft. Since

$I = \frac{\pi}{64} \left[(d_o)_{stiff}^4 - d_i^4 \right]$ where $(d_o)_{stiff}$ is the outer shaft diameter and d_i is the inner diameter, any variation in E can be accounted for by changing $(d_o)_{stiff}$ (see "Rotor Data").

2. DENST gives the weight density of the shaft material in lbs/inch³. The program converts it into the mass density $\rho = DENST/386.069$. If the density actually changes along the rotor it should be noted that the weight of the shaft per unit

length is $\rho \frac{\pi}{4} \left[(d_o)_{mass}^2 - d_i^2 \right]$ where $(d_o)_{mass}$ is the outer shaft diameter (see "Rotor Data"). Thus, $(d_o)_{mass}$ can be changed to absorb the changes in density.

3. SHM gives the product αG where G is the shear modulus, lbs/inch², and α is the shape factor for shear (for circular cross-sections: $\alpha \approx 0.75$).

Rotor Data (8E9.2)

The rotor is represented by a number of stations connected by shaft sections of uniform diameter. Thus, rotor stations are introduced wherever the shaft diameter changes (or changes significantly). Also, there must be a rotor station at each end of the rotor, at each bearing centerline and at any thrust bearing. Furthermore, a rotor station is introduced wherever the shaft has a concentrated mass which cannot readily be represented in terms of an inner and outer shaft diameter (impellers, turbine wheels, alternator poles, and so on). In this way the rotor is assigned a total of NS stations (card 2, item 1) which are numbered consecutively starting from one end of the rotor. There can be a maximum of 100 stations. Each station can be assigned a concentrated mass m with a polar mass moment of inertia I_p and a transverse mass moment of inertia I_T (any of these quantities may, of course, be zero). Also, each station can be assigned a shaft section with which it is connected to the following station. This shaft section has a length l , and outer diameter $(d_o)_{stiff}$, an outer diameter $(d_o)_{mass}$ and an inner diameter d_i . The outer diameter $(d_o)_{stiff}$ is used to spec-

ify the stiffness of the shaft section such that the cross-sectional moment of inertia of the shaft is: $I = \frac{\pi}{64} \left[(d_o)_{stiff}^4 - d_i^4 \right]$ and the shear area is:

$\frac{\pi}{4} \left[(d_o)_{stiff}^2 - d_i^2 \right]$. The outer diameter $(d_o)_{mass}$ is used in calculating the mass of the shaft such that the mass per unit length is: $\rho \frac{\pi}{4} \left[(d_o)_{mass}^2 - d_i^2 \right]$ where ρ is the mass density (see card 3, item 2).

In the computer input there must be a card for each rotor station (NS cards). Each card specifies the 7 values for the station:

1. The concentrated mass: m , lbs. (may be zero).

2. The polar mass moment of inertia of the station mass; I_p lbs-inch² (may be zero).

3. The transverse mass moment of inertia of the station mass; I_T lbs-inch² (may be zero).

4. The length of the shaft section to the next station: l , inch (may be zero). For the last station, set $l = 0$.

5. The outer diameter, $(d_o)_{stiff}$ of the shaft section, inch. $(d_o)_{stiff}$ is used in calculating the stiffness of the shaft section, $(d_o)_{stiff} \neq 0$. For the last station, set $(d_o)_{stiff} = 1.0$.

6. The outer diameter, $(d_o)_{mass}$ of the shaft section, inch (may be zero). $(d_o)_{mass}$ is used in calculating the mass of the shaft section. For the last station, set $(d_o)_{mass} = 0$.

7. The inner diameter, d_i of the shaft section, inch (may be zero). d_i is used both in calculating the stiffness and the mass of the shaft section. For the last station, set $d_i = 0$.

Bearing Stations (14I5)

The rotor station numbers at which there are bearings, are listed in sequence. This includes both journal bearings and any thrust bearings. There can be up to 10 bearings.

Pedestal Data (1P6E12.5)

The program provides for the option that the pedestals supporting the bearings may be flexible. In that case, data for the pedestals must be given and NPST must be set equal to 1 (card 2, item 3). If the pedestals are rigid, set NPST = 0 and omit giving any data for the pedestals.

When NPST = 1, each bearing is supported in a "two-dimensional" pedestal. The pedestal is represented as two separate masses, each mass on its own spring and dashpot. The one mass-spring-dashpot system represents the pedestal characteristics in the x-direction, (the vertical direction) and the other system represents the y-direction (the horizontal direction). There is no coupling between the two systems. In the computer input there must be one card for each rotor bearing and each card contains the 6 items necessary to specify the pedestal characteristics:

1. The pedestal mass for the x-direction, lbs.
2. The pedestal stiffness for the x-direction, lbs/inch.
3. The pedestal damping coefficient for the x-direction, lbs-sec/inch.
(Note: For the bearing films the damping is given in lbs/inch, whereas the damping coefficient in lbs-sec/inch is used for the pedestals).
4. The pedestal mass for the y-direction, lbs.
5. The pedestal stiffness for the y-direction, lbs/inch.

6. The pedestal damping coefficient for the y-direction, lbs-sec/inch.

When the bearings also have angular stiffness (i.e., NANG = 1, item 4, card 2) and the pedestals are flexible (i.e., NPST = 1), the above NB cards must be followed by additional NB cards, one for each bearing, on which are specified the dynamic model of the pedestals for angular motion. Each card contains six values:

1. The pedestal mass moment of inertia in the x-plane (around the y-axis), lbs-inch².

2. The pedestal angular stiffness in the x-plane (around the y-axis), lbs. inch/radian.

3. The pedestal angular damping coefficient in the x-plane (around the y-axis), lbs-inch-sec/radian.

4. The pedestal mass moment of inertia in the y-plane (around the x-axis) lbs-inch².

5. The pedestal angular stiffness in the y-plane (around the x-axis), lbs. inch/radian.

6. The pedestal angular damping coefficient in the y-plane (around the x-axis), lbs-inch-sec/radian.

Whirl Frequency Ratios (1P6E12.5)

When the rotor becomes unstable it whirls in a closed orbit with an angular frequency ν which normally is equal to approximately one half the rotational frequency ω . However, the exact value depends on the rotor and the supporting bearings, and to determine this the program searches for the zero points of the stability determinant. The present input list gives NFR values (card 2, item 5) in sequence of the whirl frequency ratio ν/ω and these values are used

directly by the program in computing the stability determinant. Thus, the program is unable to detect any possible solution outside the specified range. Furthermore, a zero point of the determinant is only detected when the determinant changes sign from one calculation to the next. Hence, if there are two zero points between two consecutive frequency ratios, the program is unable to find them. It is, therefore, necessary to make the increments sufficiently small (approximately 0.01 or less). This is most readily done by giving, say 5 or 6 frequency ratios in the present input list, and then specify an additional subdivision of the intervals by means of NIT, item 7, card 2. As an example, the present list may give 6 values for the frequency ratio: 0.7, 0.6, 0.51, 0.49, 0.4, 0.3 (NFR = 6). In addition, NIT may be set equal to 5. Thereby, the stability determinant is computed at the following 26 frequency ratios: 0.7, 0.68, 0.66, 0.64, 0.62, 0.6, 0.582, 0.564, 0.546, 0.528, 0.51, 0.506, 0.502, 0.498, 0.494, 0.49, 0.472, 0.454, 0.436, 0.418, 0.40, 0.38, 0.36, 0.34, 0.32 and 0.30. Whenever the determinant changes sign, its value is also computed at the mid-point of the interval and these three values are then used to compute the zero point by quadratic interpolation. A second quadratic interpolation is employed to get a more accurate solution.

Speed Data (1P6E12.5)

This data and the following bearing data must be repeated NCAL times (item 9, card 2). The speed data is given on one card with three values:

1. The initial speed of the speed range, rpm
2. The final speed of the speed range, rpm
3. The speed increment, rpm.

Thus, the first calculation is performed at a rotor speed equal to the initial speed. Thereafter, the speed is incremented by the speed increment, and this is repeated until reaching the final speed. The zero points of the instability determinant are found for each speed and by plotting the results as previously

discussed, the rotor speed can be determined at which instability sets in. The selected speed range should, therefore, be sufficiently large that it includes the threshold speed.

Bearing Data (8E9.2)

Each bearing is represented by 8 dynamic coefficients for radial motion such that the dynamic bearing reactions can be expressed by means of Eq. (1) (or more correctly, by Eq. (5)). The 8 coefficients are given on one card:

$$K_{xx} \quad K_{xy} \quad K_{yx} \quad K_{yy} \quad \omega B_{xx} \quad \omega B_{xy} \quad \omega B_{yx} \quad \omega B_{yy} \quad \text{lbs/inch}$$

where ω is the angular speed, radians/sec, and the 8 coefficients are computed from the lubrication equation (Reynolds equation) as described in volumes III and VII. When the lubricant is incompressible ($INC = 0$, card 2, item 6) the coefficients are independent of whirl frequency and only one set of values should be given. When the lubricant is compressible ($INC \neq 0$), the coefficients are frequency dependent and one set of coefficients must be given for each of the whirl frequency ratios in the input list, i.e. a total of NFR cards (card 2, item 5). The cards must be given in the same sequence as the values in the frequency ratio list.

When, in the search for the zero points of the instability determinant, the program performs calculations at frequency ratios different from the specified values, the proper dynamic coefficients are obtained by quadratic interpolation of the input data. Hence, a minimum of 3 sets of coefficients is required when $INC \neq 0$, which means $NFR \geq 3$. When $INC = 0$, interpolation is, of course, not necessary and only one set of coefficients is required.

If $NANG = 0$ (card 2, item 4) the above data is repeated for the next bearing until the coefficients are specified for all NB bearings. If $NANG \neq 0$, the above data is followed by a similar set of data of dynamic coefficients for angular motion. Let the dynamic moment acting on the rotor have the components M_x and M_y where M_x is in the x-z plane and M_y is in the y-z plane (z is the

coordinate along the rotor axis). The rotor amplitudes are x and y and the corresponding rotor slopes are: $\theta = dx/dz$ and $\phi = dy/dz$. The equations defining the angular dynamic coefficients are:

$$M_x = -G_{xx} \theta - D_{xx} \frac{d\theta}{dt} - G_{xy} \phi - D_{xy} \frac{d\phi}{dt} \quad (34)$$

$$M_y = -G_{yx} \theta - D_{yx} \frac{d\theta}{dt} - G_{yy} \phi - D_{yy} \frac{d\phi}{dt}$$

where t is time. These equations are completely analogous to Eq. (1). The 8 coefficients apply to a given bearing geometry, a known static bearing load and are functions of the rotor speed. For compressible lubricants, the coefficients also depend on the whirl frequency ratio such that Eq. (34) more properly should be written:

$$M_x = -Y_{xx} \theta - Y_{xy} \phi \quad (35)$$

$$M_y = -Y_{yx} \theta - Y_{yy} \phi$$

where:

$$Y_{xx} = G_{xx} + i \left(\frac{v}{\omega} \right) \omega D_{xx} \quad (36)$$

and similarly for Y_{xy} , Y_{yx} and Y_{yy} . Eq. (35) is analogous to Eq. (5) and is derived in the same way.

In the computer input, the 8 coefficients are given on one card:

$$G_{xx} \quad G_{xy} \quad G_{yx} \quad G_{yy} \quad \omega D_{xx} \quad \omega D_{xy} \quad \omega D_{yx} \quad \omega D_{yy} \quad \text{lbs.inch/radian}$$

In complete analogy to the input for the radial dynamic coefficients, only one

set of coefficients is required for an incompressible lubricant ($INC = 0$) whereas NFN cards are required for a compressible lubricant ($INC \neq 0$).

When all the required input, both the radial coefficients and the angular coefficients, has been given for one bearing, the input is repeated for the next bearing until all NB bearings are specified.

Whereas a journal bearing usually has both radial and angular coefficients, a thrust bearing has only angular coefficients and its radial coefficients should be set equal to zero. In general, the angular coefficients for a journal bearing are of minor importance and may be set equal to zero except in unusual circumstances.

COMPUTER OUTPUT

Referring to the sample calculation given later it is seen that the first couple of pages of computer output lists the input data. Thus, any mistake in the input data is readily found.

The listing in the output of the bearing data gives the 8 dynamic bearing coefficients for radial and angular motion. The angular coefficients are identified as "ANG.KXX", meaning G_{xx} , "ANG.W.BXX", meaning ωD_{xx} , and so on. The first column in the list gives the whirl frequency ratio at which the coefficients apply. For an incompressible lubricant, the coefficients are independent of frequency but to simplify the output routine a value of the frequency ratio is still given although it has no particular meaning.

After the listing of the input, follow the results of the calculations. There is a list of output for each rotor speed. The list is preceded by a title giving the rotor speed in rpm, and then follows a four column list of results. The first column gives the whirl frequency ratio ν/ω , the second column is the corresponding frequency ν , radians/sec, the third column is the real part of the instability determinant, and the fourth column is the imaginary part of the determinant.

The purpose of the calculations is to determine those frequency ratio values at which either the real part or the imaginary part of the instability determinant are zero. The program does this in the following way: to illustrate, assume that the real part is positive at a frequency ratio of 0.51 but becomes negative at the next frequency ratio in the sequence, say 0.50. Then the program calculates the determinant at the midpoint of the interval (i.e. at $\nu/\omega = 0.505$) and through these three values of the determinant (at $\nu/\omega = 0.51, 0.505$ and 0.50), it passes a second order polynomial and calculates where it becomes zero. Let this be at $\nu/\omega = 0.5024230$. This represents a "first solution". To improve the accuracy, an additional calculation is performed with $\nu/\omega = 0.5024230$, and the corresponding determinant value is used together with two neighboring values to compute a "second solution" which, then, is taken as the final solution. Obviously, the corresponding determinant is not exactly zero but it is usually 10^{-6} to 10^{-8} of the neighboring values. To spot the solutions in the list of output, simply go through the column of frequency ratios and each time the results show that an interpolation takes place, the finally obtained frequency ratio is a solution. By checking in the columns for the real part and the imaginary part of the instability determinant, it is readily found which part has a zero point.

INPUT FORM FOR COMPUTER PROGRAM

PN400: THE THRESHOLD OF INSTABILITY FOR A FLEXIBLE ROTOR IN FLUID FILM BEARINGS

Card 1 (72H) Text

Card 2 (14I5)

1. NS = Number of rotor stations ($1 \leq NS \leq 100$)
2. NB = Number of bearings ($1 \leq NB \leq 10$)
3. NPST = 0: rigid pedestals
 = 1: flexible pedestals
4. NANG = 0: no angular bearing stiffness
 = 1: bearings (and pedestals if NPST \neq 0) have angular
 stiffness
5. NFR = Number of input values of frequency ratio ($3 \leq NFR \leq 50$)
6. INC = 0: bearing lubricant is incompressible (liquid)
 = 1: bearing lubricant is compressible (gas)
7. NIT = Number of subdivisions of frequency ratio intervals ($1 \leq NIT$)
8. METR = 0: no diagnostic METR = 0 1: diagnostic
9. NCAL = Number of speed ranges
10. INP = 0: more input follows, starting with card 1
 = 1: last set of input data

Card 3 (1P6E12.5)

1. YM = Youngs modulus for shaft material, lbs/inch²
2. DENST = Weight density of shaft material, lbs/inch³
3. SHM = αG , where G is shear modulus, lbs/inch², and α is shape
 factor for shear

Rotor Data (8E9.2)

Give NS cards with 7 values on each card:

1. Weight at rotor station, lbs.
2. Polar mass moment of inertia at rotor station, lbs.inch²
3. Transverse mass moment of inertia at rotor station, lbs.inch²
4. Length of shaft section to next station, inch
5. Outer shaft diameter for cross-sectional moment of inertia, inch
6. Outer shaft diameter for shaft mass, inch
7. Inner shaft diameter, inch

Bearing Stations (14I5)

List the NB rotor stations at which there are bearings

Pedestal Data (1P6E12.5)

This data only applies when NPST \neq 0 (card 2, item 3). Give NB cards with 6 values per card, one card per bearing:

1. Pedestal vibratory mass, x-direction, lbs.
2. Pedestal stiffness, x-direction, lbs/inch
3. Pedestal damping coefficient, x-direction, lbs.sec/inch
4. Pedestal vibratory mass, y-direction, lbs.
5. Pedestal stiffness, y-direction, lbs/inch
6. Pedestal damping coefficient, y-direction, lbs.sec/inch

If also NANG \neq 0 (card 2, item 4), give additional NB cards, 6 values per card

1. Pedestal vibratory mass moment of inertia, x-plane, lbs.inch²
2. Pedestal angular stiffness, x-plane, lbs.inch/radian
3. Pedestal angular damping coefficient, x-plane, lbs.inch.sec/radian
4. Pedestal vibratory mass moment of inertia, y-plane, lbs.inch²
5. Pedestal angular stiffness, y-plane, lbs.inch/radian
6. Pedestal angular damping coefficient, y-plane, lbs.inch.sec/radian

Whirl Frequency Ratios (1P6E12.5)

List NFR values of the whirl frequency ratio in sequence, 6 values per card

Note: The remaining data must be repeated NCAL times

Speed Data (1P6E12.5)

1. Initial speed, rpm
2. Final speed, rpm
3. Speed increment, rpm

Bearing Data (8E9.2)

Give NFR cards if INC \neq 0, or 1 card only if INC = 0, with 8 dynamic translatory coefficients per card:

K_{xx} K_{xy} K_{yx} K_{yy} ωB_{xx} ωB_{xy} ωB_{yx} ωB_{yy} lbs/inch

If also NANG \neq 0, this data is followed by NFR or 1 card with 8 dynamic angular coefficients per card:

G_{xx} G_{xy} G_{yx} G_{yy} ωD_{xx} ωD_{xy} ωD_{yx} ωD_{yy} lbs.inch/radian

There is one set of coefficients per bearing, i.e. the above bearing data is repeated NB times.

```

C   DIMENSION RM( 80),RIP( 80),RIT( 80),RL( 80),RS( 80),RW( 80),
    PN400=STABILITY INHESMOLU OF FLEXIBLE ROTOR
    IRD( 80),RJ( 80),DVA( 80),DMA( 80),DMB( 80),A1( 80),A2( 80),
    2A3( 80),A4( 80),A5( 80),A6( 80),A7( 80),A8( 80),A9( 80),A10( 80),
    3FRU1(40),XL(4),SL(4),ML(4),JL(4),XR(4),SR(4),BR(4),VR(4),LB(10)
    DIMENSION PMX(2,10),PKA(2,10),PDX(2,10),PMY(2,10),PKY(2,10),
    1PDY(2,10),SB(2,8)
    DIMENSION DC(8,40,10),DA(8,40,10),DV(2,8,10)
    COMMON AC(4,4),AS(4,4),DIC,DIS
200  READ(5,100)
    READ(5,101) NS,NP,NPSI,NANG,NFR,INC,NIT,METR,NCAL,IMP
    READ(5,102) YF,DENST,SMH
    WRITE(6,100)
    WRITE(6,103)
    WRITE(6,104) NS,ND,NPSI,NANG,NFR,INC,NIT,METR,NCAL,IMP
    WRITE(6,105)
    WRITE(6,106) YF,DENST,SMH
    WRITE(6,107)
    WRITE(6,108)
    DO 201 J=1,NS
    READ(5,109) RM(J),RIP(J),RIT(J),RL(J),RS(J),RW(J),RD(J)
201  WRITE(6,110) J,RM(J),RIP(J),RIT(J),RL(J),RS(J),RW(J),RD(J)
    READ(5,101) (LR(J),J=1,NS)
    WRITE(6,111)
    WRITE(6,101) (LR(J),J=1,NS)
202  AMS=366.064
    AMSL=0.000001
204  RS(NS)=1.0
    DENST=DENST/AMS
    DO 210 J=1,NS
    RM(J)=RM(J)/AMS
    RIP(J)=RIP(J)/AMS
    RIT(J)=RIT(J)/AMS
    C2=RD(J)
    C3=RS(J)
    RS(J)=0.049087345*YF*((C3**4)-(C2**4))
    C4=RW(J)
    RW(J)=0.78539816*(C4**4-C2**2)*DENST
    IF(C4) 205,205,205
205  RJ(J)=0.0
    GO TO 207
206  RJ(J)=(C4**4+C2**2)/37.0
207  C2=1.5707963*SMH*((C3**4)-C2**2)
    IF(C2) 208,209,204
208  RD(J)=RS(J)/C2
    GO TO 210
209  RD(J)=0.0
210  CONTINUE
    IF(NPSI) 211,215,211
211  WRITE(6,112)
    WRITE(6,113)
    DO 212 J=1,NS
    READ(5,102) PKA(1,J),PKA(1,J),PDX(1,J),PMY(1,J),PKY(1,J),
    1PDY(1,J)
    WRITE(6,110) LR(J),PKA(1,J),PKA(1,J),PDX(1,J),PMY(1,J),PKY(1,J),
    1PDY(1,J)
    PMX(1,J)=PMX(1,J)/AMS
212  PMY(1,J)=PMY(1,J)/AMS
    IF(NANG) 213,215,213
213  WRITE(6,114)
    DO 214 J=1,NS
    READ(5,102) PMX(2,J),PKA(2,J),PDX(2,J),PMY(2,J),PKY(2,J),
    1PDY(2,J)
    WRITE(6,110) LR(J),PKA(2,J),PKA(2,J),PDX(2,J),PMY(2,J),PKY(2,J),
    1PDY(2,J)
    PMX(2,J)=PMX(2,J)/AMS
214  PMY(2,J)=PMY(2,J)/AMS

```

215	READ(5,102) (FRQ1(J);J=1,NFR)	
	WRITE(6,115)	
	WRITE(6,106) (FRQ1(J),J=1,NFR)	
	IC=1	70
301	READ(5,102) SPST,SPFN,SPNC	
	K1=NFR	72
	IF(INC) 303,302,303	73
302	K1=1	74
303	WRITE(6,116)	
	WRITE(6,106) SPST,SPFN,SPNC	
	WRITE(6,117)	
	DO 310 K=1,NH	78
	WRITE(6,118) LK(K)	
	WRITE(6,119)	
	DO 306 J=1,K1	81
	READ(5,109) (DC(I,J,K),I=1,8)	
306	WRITE(6,121) FRQ1(J), (DC(I,J,K),I=1,8)	
	IF(NANG) 307,310,307	84
307	WRITE(6,120)	
	DO 308 J=1,K1	86
	READ(5,109) (CA(I,J,K),I=1,8)	
308	WRITE(6,121) FRQ1(J), (CA(I,J,K),I=1,8)	
310	CONTINUE	89
	SPD=SPSI	90
320	ANSP=0.10471976*SPD	91
	WRITE(6,122) SPD	
	WRITE(6,123)	
	IO=1	94
	FRW=FRQ1(1)	95
	KR=0	96
	KE=0	97
	K1=1	98
	K2=0	99
	K3=0	100
	DFW=NIT	101
	DFW=(FRQ1(2)-FRW)/LX*	102
325	FRQ=ANSP*FRW	103
	FRQ2=FRQ*FRQ	104
	DO 326 J=1,N5	105
	DVA(J)=FRQ2*PV(J)	106
	DMA(J)=-FRQ2*MIT(J)	107
326	DMR(J)=FRQ*ANSP*MIT(J)	108
330	DO 375 J=1,NH	109
	IF(INC) 332,331,332	110
331	I1=1	111
	GO TO 334	112
332	IF(K2) 335,333,334	113
333	I1=I0	114
334	DO 336 I=1,8	115
	SH(I,I)=DC(I,I1,J)	116
	IF(NANG) 337,335,335	117
335	SH(2,I)=CA(I,I1,J)	118
336	CONTINUE	119
	GO TO 339	120
338	I1=I0	121
	I2=2	122
	I3=0	123
	IF(K3) 340,340,339	124
339	I1=I0+1	125
340	IF(NFR=I1) 356,356,341	126
341	C4=FRQ1(I1)	127
	C1=FRQ1(I1+1)-C4	128
	C2=C4-FRQ1(I1-1)	129
	C3=C1+C2	130
	C4=FRW-C4	131
	DO 355 I=1,8	132
	C5=DC(I,I1,J)	133
	C6=(DC(I,I1+1,J)-C5)/(C1*C3)	134
	CR=(DC(I,I1-1,J)-C5)/(C2*C3)	135

	C7=C6+C8	136
	C6=C2*C6-C1*C8	137
	C8=C5+C9*(C6+C9+C7)	138
	IF(I1-I2) 343,342,343	139
342	SB(1,I)=C8	140
	IF(NANG) 347,355,347	141
343	IF(I3) 344,344,345	142
344	SB(1,I)=C8/C2*(FRW-FRW1(I1-1))	143
	IF(NANG) 347,355,347	144
345	SB(1,I)=SB(1,I)+C8/C1*(FRQ1(I1+1)-FRW)	145
	IF(NANG) 347,355,347	146
347	C5=DA(1,I1,J)	147
	C6=(DA(1,I1+1,J)-C5)/(C1*CJ)	148
	C8=(DA(1,I1-1,J)-C5)/(C2*CJ)	149
	C7=C6+C8	150
	C6=C2*C6-C1*C8	151
	C8=C5+C9*(C6+C9+C7)	152
	IF(I1-I2) 349,349,349	153
348	SB(2,I)=C8	154
	GO TO 355	155
349	IF(I3) 350,350,352	156
350	SB(2,I)=C8/C2*(FRW-FRW1(I1-1))	157
	GO TO 355	158
352	SB(2,I)=SB(2,I)+C8/C1*(FRW1(I1+1)-FRW)	159
355	CONTINUE	160
356	IF(I3) 359,357,359	161
357	IF(I1-I2) 359,359,358	162
358	I1=I1-1	163
	I2=NFR-1	164
	I3=1	165
	GO TO 341	166
359	DO 360 I=1,M	167
	DV(1,I,J)=0.0	168
360	DV(2,I,J)=0.0	169
	I1=1	170
361	DO 362 I=5,M	171
362	SB(1,I)=FRW*SB(1,I)	172
	IF(NPST) 365,363,365	173
363	DO 364 I=1,M	174
364	DV(1,I,J)=SB(1,I)	175
	GO TO 370	176
365	C1=PKX(I1,J)-FRQ2*PKX(I1,J)	177
	C2=FRQ*PKX(I1,J)	178
	C3=PKY(I1,J)-FRQ2*PKY(I1,J)	179
	C4=FRQ*PKY(I1,J)	180
	C5=SB(1,1)+C1	181
	C6=SB(1,5)+C2	182
	C7=SB(1,4)+C3	183
	C8=SB(1,8)+C4	184
	D1=C5*C7-C6*C8-SB(1,2)*SB(1,3)+SB(1,6)*SB(1,7)	185
	D2=C5*C4+C6*C7-SB(1,2)*SB(1,7)-SB(1,3)*SB(1,6)	186
	IF(ABS(D1)-ABS(D2)) 367,366,366	187
366	D3=D2/D1	188
	D4=D1+D3*D2	189
	D1=1.0/D4	190
	D2=-D3*D1	191
	GO TO 368	192
367	D3=D1/D2	193
	D4=D2+D3*D1	194
	D2=-1.0/D4	195
	D1=-D3*D2	196
368	D3=C1*D1-C2*D2	197
	D4=C1*D2+C2*D1	198
	D5=1.0-D3*C7+D4*C8	199
	D6=-D3*C8-D4*C7	200
	DV(1,1,J)=C1*D5-C2*D6	201
	DV(1,5,J)=C1*D6+C2*D5	202
	D5=C3*SB(1,2)-C4*SB(1,6)	203
	D6=C4*SB(1,2)+C3*SB(1,6)	204

DV(11.2,J)=D3*D5-D4*D6	205
DV(11.6,J)=D3*D6+D4*D5	206
D5=C3*SH(11.3)-C4*SH(11.7)	207
D6=C4*SH(11.3)+C3*SH(11.7)	208
DV(11.3,J)=D3*D5-D4*D6	209
DV(11.7,J)=D3*D6+D4*D5	210
D3=C3*D1-C4*D2	211
D4=C3*D2+C4*D1	212
D5=1.0-D3*C5+D4*C6	213
D6=-D3*C6-D4*C5	214
DV(11.4,J)=C3*D5-C4*D6	215
DV(11.8,J)=C3*D6+C4*D5	216
370 IF(NANG) 371,375,371	217
371 IF(11-1) 372,372,375	218
372 11=2	219
GO TO 361	220
375 CONTINUE	221
IF(METN) 381,382,382	222
381 11=IAHS*(MFR)	223
WRITE(6,121)FRN,(DV(11.1,1),1=1,3	
GO TO 400	225
382 CONTINUE	226
11=NS-1	227
DO 420 J=1,11	228
C1=RS(J)	229
C2=FR02*RW(J)	230
C3=RU(J)	231
C10=KJ(J)	232
C4=C2/C1	233
C5=SQRT(C4)	234
C6=SQRT(C5)	235
C7=RL(J)	236
IF(C6*C7-0.03) 411,411,412	237
411 C8=C2*C7	238
D1=C7*C7*C4	239
D2=C7*D1	240
D3=C7*U2	241
D4=D1*(C3-C10)	242
D5=C7/C1	243
D6=C7*U5/2.0	244
D7=C7*U5/3.0	245
D8=C3-C10	246
D8=D8*D8+C3*C10	247
A1(J)=1.0+D3/24.0	248
A2(J)=A1(J)-04	249
A3(J)=(1.0-04/3.0+03/120.0)*C7	250
A4(J)=02/6.0	251
A5(J)=C1*A4(J)	252
A6(J)=C2*A3(J)	253
A7(J)=(1.0+2.0*C4*C3*(10+D3/120.0)*D5	254
A7(J)=1.0-04/3.0+03/120.0	255
A7(J)=C8*RW(J)/2.0*C7	256
BN(J)=D5*RW(J)	257
DN(J)=(1.0+4.0*C4*D8)*D7-(C3-C10)*2.0*D5	258
GO TO 420	259
412 C9=(4*(C3+C10)**2)	260
C9=C5*(C3-C10)	261
IF(C9-0.0002) 413,413,414	262
413 C11=1.0+0.25*D5	263
C8=1.0+0.5*C8	264
GO TO 415	265
414 C8=SQRT(1.0+C8)	266
C11=SQRT(C8)	267
415 D5=C5*(C8*(C9))	268
D6=C5*(C8*(C9))	269
D9=D5+D6	270
IF(ABS(C9/C8)-0.0002) 416,416,417	271

416	D8=0.5/C8*C9	272
	D3=C8*C11*(1.0-D8)	273
	D4=C6*C11*(1.0-D8)	274
	GO TO 41e	275
417	D3=SQRT(D5)	276
	D4=SQRT(D6)	277
418	D7=D3*D5	278
	DA=D4*D6	279
	D1=D3*C7	280
	D2=D4*C7	281
	VC=COS(D2)/D9	282
	VS=SIN(D2)/D9	283
	BMC=EXP(D1)	284
	BMS=1.0/BMC	285
	D1=0.5*(BMC+BMS)/D9	286
	D2=0.5*(BMC-BMS)/D9	287
	A1(J)=D4*D1+D5*VC	288
	A2(J)=D5*D1+D6*VC	289
	A3(J)=D3*D2+D4*VS	290
	A6(J)=C2*A3(J)	291
	BN(J)=(D1-VC)/C1	292
	A7(J)=C2*(D1-VC)	293
	A4(J)=C5*(D4*D2-D3*VS)	294
	A5(J)=C1*A4(J)	295
	CA=C1*C5	296
	AN(J)=(D6*D2+D7*VS)/C8	297
	DN(J)=(D7*D2-D8*VS)/C8	298
420	CONTINUE	299
	DO 470 I=1,4	300
	DO 452 J=1,4	301
	XL(J)=0.0	302
	SL(J)=0.0	303
	HL(J)=0.0	304
452	VL(J)=0.0	305
	I1=I+I-1	306
	IF(I-2) 453,453,454	307
453	XL(I1)=AMSL	308
	GO TO 455	309
454	I1=I1-4	310
	SL(I1)=AMSL	311
455	I1=1	312
	I2=LH(I)	313
	DO 465 J=1,NS	314
	DO 456 L=1,4	315
	HR(L)=HL(L)+DMA(J)*SL(L)	316
	VR(L)=VL(L)+DVA(J)*XL(L)	317
	XR(L)=XL(L)	318
456	SR(L)=SL(L)	319
	BR(1)=BR(1)+DMA(J)*SL(4)	320
	BR(2)=BR(2)+DMA(J)*SL(3)	321
	BR(3)=BR(3)+DMA(J)*SL(2)	322
	BR(4)=BR(4)+DMA(J)*SL(1)	323
	IF(I2-J) 460,457,460	324
457	BR(1)=BR(1)+SL(1)*DV(2,1,I1)-SL(2)*DV(2,5,I1)+SL(3)*DV(2,2,I1)-	325
	1SL(4)*DV(2,6,I1)	326
	BR(2)=BR(2)+SL(1)*DV(2,5,I1)+SL(2)*DV(2,1,I1)+SL(3)*DV(2,6,I1)+	327
	1SL(4)*DV(2,2,I1)	328
	BR(3)=BR(3)+SL(1)*DV(2,3,I1)-SL(2)*DV(2,7,I1)+SL(3)*DV(2,4,I1)-	329
	1SL(4)*DV(2,8,I1)	330
	BR(4)=BR(4)+SL(1)*DV(2,7,I1)+SL(2)*DV(2,3,I1)+SL(3)*DV(2,8,I1)+	331
	1SL(4)*DV(2,4,I1)	332
	VR(1)=VR(1)-XL(1)*DV(1,1,I1)+XL(2)*DV(1,5,I1)-XL(3)*DV(1,2,I1)+	333
	1XL(4)*DV(1,6,I1)	334
	VR(2)=VR(2)-XL(1)*DV(1,5,I1)-XL(2)*DV(1,1,I1)-XL(3)*DV(1,6,I1)-	335
	1XL(4)*DV(1,2,I1)	336
	VR(3)=VR(3)+XL(1)*DV(1,3,I1)+XL(2)*DV(1,7,I1)-XL(3)*DV(1,4,I1)+	337
	1XL(4)*DV(1,8,I1)	338
	VR(4)=VR(4)-XL(1)*DV(1,7,I1)-XL(2)*DV(1,3,I1)-XL(3)*DV(1,8,I1)-	339
	1XL(4)*DV(1,4,I1)	340

	I1=I1+1	341
	IF(NH=1) 458,459,459	342
458	I2=NS+2	343
	GO TO 460	344
459	I2=L4(I1)	345
460	IF(NS=J) 465,465,461	346
461	DO 462 L=1,4	347
	XL(L)=A2(J)*X(L)+A3(J)*SH(L)+AN(J)*HR(L)+DN(J)*VR(L)	348
	SL(L)=A4(J)*X(L)+A1(J)*SH(L)+AN(J)*BR(L)+BN(J)*VR(L)	349
	BL(L)=A7(J)*X(L)+A5(J)*SH(L)+A1(J)*HR(L)+A3(J)*VR(L)	350
462	VL(L)=AN(J)*X(L)+A7(J)*SH(L)+A4(J)*BR(L)+A2(J)*VR(L)	351
465	CONTINUE	352
	AC(1,1)=VM(1)	353
	AC(2,1)=VM(3)	354
	AC(3,1)=BK(1)	355
	AC(4,1)=BK(3)	356
	AS(1,1)=VM(2)	357
	AS(2,1)=VM(4)	358
	AS(3,1)=BK(2)	359
	AS(4,1)=BK(4)	360
470	CONTINUE	361
	CALL CUEIN	
	WRITE(6,105)FRW,FRW,DFW,DFW	
	IF(KH) 456,456,455	364
480	IF(KH) 507,491,507	365
481	IF(K1) 473,483,482	366
482	K1=0	367
	DC1=DTC	368
	TC1=FRW	369
	GO TO 486	370
483	IF(DTC=DC1) 470,470,470	371
484	DC1=DTC	372
	TC1=FRW	373
485	IF(DTS=DS1) 505,485,486	374
486	DS1=DTS	375
	TS1=FRW	376
	IF(NH=16) 550,550,487	377
487	IF(NIT=1-K3) 489,489,488	378
488	K3=K3+1	379
	K2=1	380
	FRW=FRW+DFW	381
	GO TO 325	382
489	K3=0	383
	K2=0	384
	I0=I0+1	385
	FRW=FRW1(I0)	386
	IF(NH=16) 490,490,491	387
490	DFW=0.1	388
	GO TO 325	389
491	DFW=NII	390
	DFW=(FRW1(I)+1)-FRW)/DFW	391
	GO TO 325	392
492	K4=1	393
	DC3=DTC	394
	TC4=FRW	395
	DS3=DTS	396
	TS4=FRW	397
	FRW=(FRW+TC1)/2.0	398
	K2=1	399
	GO TO 325	400
495	K4=-1	401
	X1=TC1	402
	X2=FRW	403
	X3=TC3	404
	Y1=DC1	405
	Y2=DTC	406
	Y3=DC3	407
	GO TO 520	408
496	IF(KH+1) 501,497,497	409

497	KR=-2	410
	IF (FRW-X2) 499,498,498	411
498	X1=X2	412
	Y1=Y2	413
	GO TO 500	414
499	X3=X2	415
	Y3=Y2	416
500	X2=FRW	417
	Y2=DTC	418
	GO TO 520	419
501	KR=0	420
	DTS=DS3	421
	FRW=TS3	422
	DC1=DC3	423
	TC1=TC3	424
	GO TO 485	425
505	KE=1	426
	DS3=DTS	427
	TS3=FRW	428
	FRW=(FRW+TS1)/2.0	429
	K2=1	430
	GO TO 325	431
506	KE=-1	432
	X1=TS1	433
	X2=FRW	434
	X3=TS3	435
	Y1=DS1	436
	Y2=DTS	437
	Y3=DS3	438
	GO TO 520	439
507	IF (KE+1) 512,508,508	440
508	KF=-2	441
	IF (FRW-X2) 510,509,509	442
509	X1=X2	443
	Y1=Y2	444
	GO TO 511	445
510	X3=X2	446
	Y3=Y2	447
511	X2=FRW	448
	Y2=DTS	449
	GO TO 520	450
512	KF=0	451
	DTS=DS3	452
	FRW=TS3	453
	GO TO 485	454
520	C1=X3-X2	455
	C2=X2-X1	456
	C3=X3-X1	457
	C4=(Y3-Y2)/(C1*C3)	458
	C4=(Y1-Y2)/(C2*C3)	459
	C5=C2*C4-C1*C6	460
	C4=C4+C6	461
	IF (C4) 522,521,522	462
521	C6=-Y2/C5	463
	GO TO 525	464
522	C5=0.5/C4*C5	465
	C4=ABS(C5*C5-Y2/C4)	466
	C4=SQR(C4)	467
	IF (C5) 523,524,524	468
523	C4=-C4	469
524	C6=C4-C5	470
525	FRW=X2+C6	471
	GO TO 325	472
550	SPD=SPD*SPIC	473
	IF (SPFN+0.00001-SPD) 552,552,320	474
552	IF (NCAL-IC) 554,554,553	475
553	IC=IC+1	476
	GO TO 321	477
554	IF (INP) 555,200,555	478

```

555 CALL EXIT
100 FORMAT(72H
1
101 FORMAT(14I5)
102 FORMAT(6E12.5)
103 FORMAT(49HSTATIONS NO.IMPUS PED.FLEX ANG.FLEX NO.FREQ INCOMPR
ISUMDIVS METRIC SPEEDS INPUT)
104 FORMAT(16.9I9)
105 FORMAT(13H0 YOUNGS MOD.5A2SDENSITY (SPEAK FACT)*6)
106 FORMAT(HE14.5)
107 FORMAT(11HROTOR DATA)
108 FORMAT(104HSTATION MASS POLAR MOM.IN. TRANSV.MOM.IN L
LENGTH OUT.DIA(STIFF) OUT.DIA(MASS) INNER DIA.)
109 FORMAT(3E9.2)
110 FORMAT(15.8I6.5.7E14.0)
111 FORMAT(17HBEARING STATIONS)
112 FORMAT(14HROTORIAL DATA)
113 FORMAT(40HSTATION MASS-X STIFFNESS-X DAMPING-X MA
ISS-Y STIFFNESS-Y DAMPING-Y)
114 FORMAT(40HSTATION MOM.INERTIA ANG.STIFFN-X ANG.DAMP-X MOM.
INERTY ANG.STIFFN-Y ANG.DAMP-Y)
115 FORMAT(23HROTORIAL FREQUENCY RATIOS)
116 FORMAT(42HINITIAL SPEED FINAL SPEED SPEED INCR.)
117 FORMAT(72H0DYNAMIC BEARING COEFFICIENTS)
118 FORMAT(72H0DYNAMIC BEARING AT ROTOR STATION13)
119 FORMAT(13H FREQ.RATIOA33KAA10X3HKA10X3HKY10X3HKYY9X5HW*8XX8X5
IHE8AYKASHA*SYA8A8H*YY)
120 FORMAT(13H FREQ.RATIOA7HANG.KAA6A7HANG.KXY6A7HANG.KYX6X7HANG.KY
1Y5X7HANG.K*8X4X4X7HANG.*8*8AY4X7HANG.*8*8Y4X7HANG.*8*8YY)
121 FORMAT(2E14.5.7E15.5)
122 FORMAT(77713H0 ROTOR SPEED=13.044H RPM)
123 FORMAT(55H0 FREQ.RATIO FREQUENCY RE(ETERM) IM(ETERM))
END
SURROUTINE COEIN
C SURROUTINE FOR PN400
DIMENSION INDX(4.3)
COMMON AC(4.4).AS(4.4).DTC.DTS
C INITIALIZATION
N=4
DTC=1.0
DTS=0.0
DO 10 J=1.4
10 INDX(J.3)=0
C CHECK FOR ZERO MATRIX
DO 15 I=1.4
IRW=1
ICL=1
DO 14 J=1.4
IF(ABS(AC(I.J))+ABS(AS(I.J))) 12.12.11
11 IRW=0
12 IF(ABS(AC(J.I))+ABS(AS(J.I))) 14.14.13
13 ICL=0
14 CONTINUE
IF(IRW+ICL) 15.15.46
15 CONTINUE
C SEARCH FOR PIVOT ELEMENT
DO 41 I=1.4
TST=0.0
DO 24 J=1.4
IF(INDX(J.3)-1) 17.24.17
17 DO 23 K=1.4
IF(INDX(K.3)-1) 13.23.46
18 C1=SQRT(AC(J.K)*AC(J.K)+AS(J.K)*AS(J.K))
IF(TST-C1) 22.23.23
22 IRW=J
ICL=K
TST=C1
23 CONTINUE

```

24	CONTINUE	33
	INDX(ICL,3)=INX(ICL,3)+1	34
	INDX(I,1)=IRW	35
	INDX(I,2)=ICL	36
C	INTERCHANGE ROWS TO PUT PIVOT ELEMENT ON DIAGONAL	37
	IF(IRW-ICL) 25,29,25	
25	DTC=-DTC	
	DTS=-DTS	
	DO 26 L=1,N	
	C1=AC(IRW,L)	40
	C2=AS(IRW,L)	41
	AC(IRW,L)=AC(ICL,L)	42
	AS(IRW,L)=AS(ICL,L)	43
	AC(ICL,L)=C1	44
26	AS(ICL,L)=C2	45
C	DIVIDE PIVOT ROW BY PIVOT ELEMENT	46
29	C1=AC(ICL,ICL)	47
	C2=AS(ICL,ICL)	48
	TST=DTC	
	DTC=C1*TST-C2*DTS	
	DTS=C2*TST+C1*DTS	
	AC(ICL,ICL)=1.0	49
	AS(ICL,ICL)=0.0	50
	IF(ABS(C1)-ABS(C2)) 31,30,30	51
30	TST=C2/C1	52
	C1=1.0/(C1+TST*C2)	53
	C2=TST*C1	54
	GO TO 32	55
31	TST=C1/C2	56
	C2=1.0/(C2+TST*C1)	57
	C1=TST*C2	58
32	DO 33 L=1,N	59
	TST=AC(ICL,L)	60
	AC(ICL,L)=C1*TST+C2*AS(ICL,L)	61
33	AS(ICL,L)=C1*AS(ICL,L)-C2*TST	62
C	REDUCE NON-PIVOT ROWS	63
36	DO 41 L1=1,N	64
	IF(L1-ICL) 37,41,37	65
37	C1=AC(L1,ICL)	66
	C2=AS(L1,ICL)	67
	AC(L1,ICL)=0.0	68
	AS(L1,ICL)=0.0	69
	DO 38 L=1,N	70
	AC(L1,L)=AC(L1,L)-C1*AC(ICL,L)+C2*AS(ICL,L)	71
38	AS(L1,L)=AS(L1,L)-C2*AC(ICL,L)-C1*AS(ICL,L)	72
41	CONTINUE	73
C	INTERCHANGE COLUMNS	74
	DO 44 I=1,N	75
	L=N+1-I	76
	IF(INDX(L,1)-INDX(L,2)) 42,44,42	77
42	IRW=INDX(L,1)	78
	ICL=INDX(L,2)	79
	DO 43 K=1,N	80
	C1=AC(K,IRW)	81
	C2=AS(K,IRW)	82
	AC(K,IRW)=AC(K,ICL)	83
	AS(K,IRW)=AS(K,ICL)	84
	AC(K,ICL)=C1	85
	AS(K,ICL)=C2	86
43	CONTINUE	87
44	CONTINUE	88
	DO 45 K=1,N	89
	IF(INDX(K,3)-1) 46,45,46	90
45	CONTINUE	91
	ID=1	92
	GO TO 47	93
46	ID=2	94
	DTC=0.0	
	DTS=0.0	
47	RETURN	95
	END	96

REFERENCES

1. Rotor-Bearing Dynamics Design Technology, Part V: "Computer Program Manual for Rotor Response and Stability," Technical Report AFAPL-TR-65-45, Part V, J. W. Lund, May 1965.
2. Rotor-Bearing Dynamics Design Technology, Part VII: "The Three Lobe Bearing and Floating Ring Bearing," Technical Report AFAPL-TR-65-45, Part VII, J. W. Lund, February 1968.
3. Rotor-Bearing Dynamics Design Technology, Part VI: "The Influence of Electromagnetic Forces on the Stability and Response of an Alternator Rotor," Technical Report AFAPL-TR-64-45, Part VI, J. W. Lund and T. Chiang, September 1967.
4. Lund, J. W., "The Stability of an Elastic Rotor in Journal Bearings with Flexible, Damped Supports", Trans. ASME, Journal of Applied Mechanics, Series E Volume 87, pp. 911-920.
5. Lund, J. W., Wernick, R. J. and Malanoski, S. B., "Analysis of the Hydrostatic Journal and Thrust Bearing for the NASA AB-5 Gyro Gimbal Bearing", Mechanical Technology Inc., Report No. MTI-62TR26, 1962.
6. Hildebrand, F.B., "Introduction to Numerical Analysis", McGraw-Hill Book C., 1956, pp. 41-43.
7. Tang, I.C. and W.A. Gross, "Analysis and Design of Externally Pressurized Gas Bearings", ASLE Paper No. 61LC-20, 1961.
8. Design of Gas Bearings, Vol. I, Mechanical Technology Inc., 1969, Section 5.6.

Unclassified

Security Classification

DOCUMENT CONTROL DATA - R & D

(Security classification of title, body of abstract and indexing annotation must be entered when the overall report is classified)

1. ORIGINATING ACTIVITY: (Corporate author) Mechanical Technology Incorporated 968 Albany-Shaker Road Latham, New York 12110		2a. REPORT SECURITY CLASSIFICATION Unclassified	
		2b. GROUP N/A	
3. REPORT TITLE Rotor-Bearing Dynamics Design Technology Part IX: Thrust Bearing Effects on Rotor-Bearing Stability			
4. DESCRIPTIVE NOTES (Type of report and inclusive dates) Final Report for Period October 1968 to January 1969			
5. AUTHOR(S) (First name, middle initial, last name) R.A. Cundiff and J. Vohr			
6. REPORT DATE August 10, 1970		7a. TOTAL NO. OF PAGES 97	7b. NO. OF REFS 8
8a. CONTRACT OR GRANT NO. AF33(615)-3228 ✓		9a. ORIGINATOR'S REPORT NUMBER(S) MTI 70TR40	
b. PROJECT NO. 3048		9b. OTHER REPORT NO.: (Any other numbers that may be assigned this report) AFAPL-TR-65-45, Part IX	
c. Task Nr: 304806			
d. Task Nr: 304806			
10. DISTRIBUTION STATEMENT This document is subject to special export controls and each transmittal to foreign governments or foreign nationals may be made only with prior approval of the Air Force Aero Propulsion Laboratory (APFL), Wright-Patterson Air Force Base, Ohio 45433.			
11. SUPPLEMENTARY NOTES None		12. SPONSORING MILITARY ACTIVITY Air Force Aero Propulsion Laboratory Wright-Patterson AFB, Ohio 45433	
13. ABSTRACT This volume presents a study conducted to determine the effects thrust bearings on rotor-bearing stability. A computer program, written in order to study these effects, permits the inclusion of the thrust bearing characteristics into the rotor system. A program manual is provided, containing a listing of the program and detailed instructions for preparation of input data. A technique is also presented which provides for the user a convenient method of evaluating the stability of a rotor system with and without the thrust bearing data. Extensive design data are presented for gas-lubricated, externally pressurized thrust bearings.			

DD FORM 1 NOV 65 1473 (PAGE 1)

S/N 0101-807-6801

Unclassified

Security Classification

Unclassified

Security Classification

14 KEY WORDS	LINK A		LINK B		LINK C	
	ROLE	WT	ROLE	WT	ROLE	WT
Bearings						
Critical Speed						
Lubrication						
Fluid Film						
Hybrid						
Hydrodynamic						
Hydrostatic						
Rotor-Bearing Dynamics						
Stability						
Stiffness and Damping						
Gas Lubrication						
Gas Bearings						

Unclassified

Security Classification